

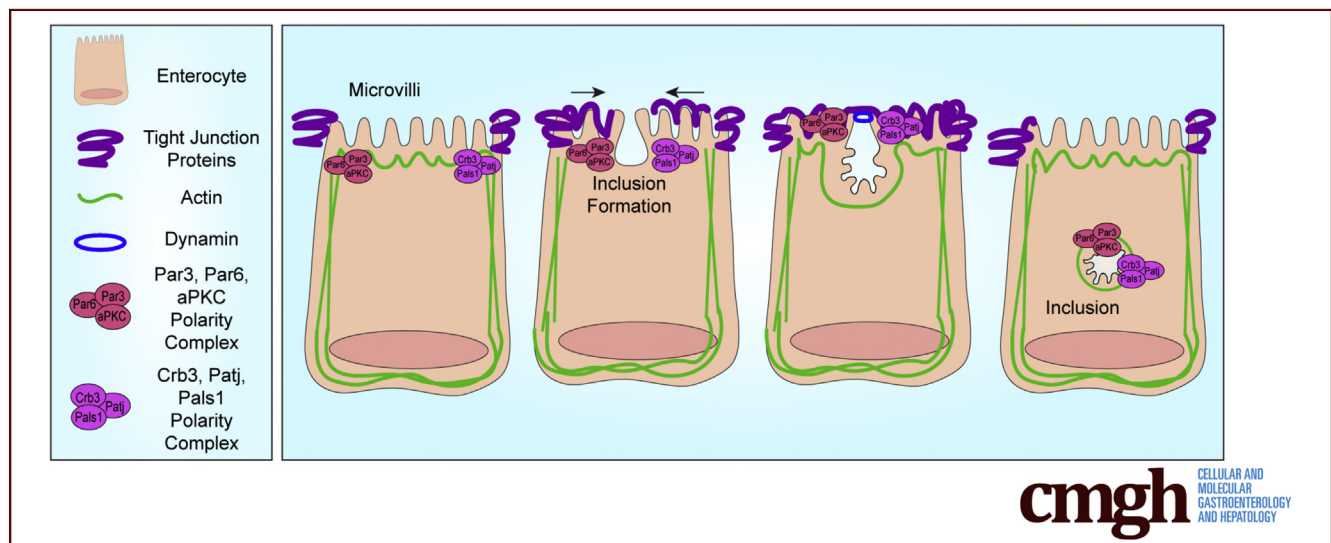
## ORIGINAL RESEARCH

## Recruitment of Polarity Complexes and Tight Junction Proteins to the Site of Apical Bulk Endocytosis



Amy C. Engevik,<sup>1,2</sup> Evan S. Krystofiak,<sup>3</sup> Izumi Kaji,<sup>1,2</sup> Anne R. Meyer,<sup>1,2,3</sup> Victoria G. Weis,<sup>1,2</sup> Anna Goldstein,<sup>1,2</sup> Alexander W. Coutts,<sup>4</sup> Tamene Melkamu,<sup>4</sup> Milena Saqui-Salces,<sup>5</sup> and James R. Goldenring<sup>1,2,3,6</sup>

<sup>1</sup>Section of Surgical Sciences, Vanderbilt University Medical Center, Nashville, Tennessee; <sup>2</sup>Epithelial Biology Center, Vanderbilt University School of Medicine, Nashville, Tennessee; <sup>3</sup>Department of Cell and Developmental Biology, Vanderbilt University, Nashville, Tennessee; <sup>4</sup>Recombinetics, Inc, Eagan, Minnesota; <sup>5</sup>Department of Animal Science, University of Minnesota, Saint Paul, Minnesota; and <sup>6</sup>Nashville VA Medical Center, Nashville, Tennessee



## SUMMARY

Loss of Myosin Vb results in intracellular inclusions that arise from endocytosis of the apical membrane in intestinal absorptive cells. Forming inclusions have a dense accumulation of tight junction proteins and are associated with apical polarity Crumbs and Par complexes.

**BACKGROUND & AIMS:** The molecular motor, Myosin Vb (MYO5B), is well documented for its role in trafficking cargo to the apical membrane of epithelial cells. Despite its involvement in regulating apical proteins, the role of MYO5B in cell polarity is less clear. Inactivating mutations in MYO5B result in microvillus inclusion disease (MVID), a disorder characterized by loss of key apical transporters and the presence of intracellular inclusions in enterocytes. We previously identified that inclusions in Myo5b knockout (KO) mice form from invagination of the apical brush border via apical bulk endocytosis. Herein, we sought to elucidate the role of polarity complexes and tight junction proteins during the formation of inclusions.

**METHODS:** Intestinal tissue from neonatal control and Myo5b KO littermates was analyzed by immunofluorescence to determine the localization of polarity complexes and tight junction proteins.

**RESULTS:** Proteins that make up the apical polarity complexes—Crumbs3 and Pars complexes—were associated with inclusions in Myo5b KO mice. In addition, tight junction proteins were observed to be concentrated over inclusions that were present at the apical membrane of Myo5b-deficient enterocytes in vivo and in vitro. Our mouse findings are complemented by immunostaining in a large animal swine model of MVID genetically engineered to express a human MVID-associated mutation that shows an accumulation of Claudin-2 over forming inclusions. The findings from our swine model of MVID suggest that a similar mechanism of tight junction accumulation occurs in patients with MVID.

**CONCLUSIONS:** These data show that apical bulk endocytosis involves the altered localization of apical polarity proteins and tight junction proteins after loss of Myo5b. (*Cell Mol Gastroenterol Hepatol* 2021;12:59–80; <https://doi.org/10.1016/j.jcmgh.2021.01.022>)

**Keywords:** Microvillus Inclusion Disease (MVID); Myosin Vb; Polarity; Tight Junctions; Inclusions; Apical Bulk Endocytosis; ZO-1; Occludin; Cortactin; Trafficking.

See editorial on page 348.

A primary function of the gut epithelium is the absorption of nutrients and water. These actions are facilitated by the proper distribution of transporters at the apical and basal membranes of intestinal epithelial cells. The establishment and maintenance of epithelial polarity are controlled by a network of protein trafficking machinery, cytoskeletal rearrangements, and polarity complexes. One key trafficking component in enterocytes is the molecular motor protein, myosin Vb (MYO5B). MYO5B interacts with the small guanosine triphosphatases Ras-related in brain (Rab) 8a and Rab11a, thereby regulating plasma membrane recycling and vesicle trafficking.<sup>1,2</sup> Although many studies have focused on epithelial polarity under homeostatic conditions, the role of MYO5B in regulating polarity remains poorly understood. Inactivating mutations in MYO5B result in microvillus inclusion disease (MVID) in newborns.<sup>3–9</sup> MVID is characterized by severe congenital diarrhea, resulting from an inability to properly absorb water coupled with active chloride secretion, which drives further dehydration.<sup>10–14</sup> The presence of intracellular inclusions containing microvilli is a hallmark of MVID.<sup>6,15</sup> We previously showed that inclusions in Myo5b-deficient enterocytes form through apical bulk endocytosis, which requires Palsin2 and Dynamin2.<sup>16</sup> Other features of MVID include the loss of, or altered, apical microvilli, improper accumulation of apical components below the brush border, and morphologic changes in the overall villi structure.<sup>4,15,17,18</sup>

Intestinal abnormalities that result from the loss of functional MYO5B have raised the question of the role of MYO5B in regulating epithelial cell polarity. Despite correlative evidence that loss of MYO5B results in altered localization of both apical and basal proteins, few studies have investigated the impact of MYO5B on the core polarity proteins and no studies to date have used experimental animal models to elucidate alterations in polarity proteins after loss of MYO5B. Interestingly, knockout (KO) models of polarity complex proteins, such as the Crumbs3 KO mice, manifest many of the same intestinal characteristics as Myo5b KO mice, including villi fusion, short and disorganized microvilli, and membrane blebbing.<sup>19,20</sup> Crumbs3 acts as a link between the apical membrane and the actin cytoskeleton.<sup>21,22</sup> Crumbs3 can bind to proteins associated with Lin-7 (Pals1) and Pals1-associated tight junction protein (Patj) to form the Crumbs3–Pals–Patj complex, which regulates epithelial cell polarization and tight junction assembly.<sup>23</sup> In addition to Pals1 and Patj, Crumbs3 also can interact with Par6 to regulate epithelial polarity and tight junctions. Par6 is a core protein that makes up the apical Par complex, which is composed of Par3–Par6–aPKC.<sup>24</sup>

Apical membrane identity in polarized cells is regulated by the localization and modulation of atypical protein kinase

C (aPKC) kinase activity by Par3 and Par6.<sup>24–26</sup> Providing a potential link between MYO5B and Par complexes, Michaux et al<sup>27</sup> showed that Par6, cell division control protein 42 homolog (Cdc42), and PKC $\zeta/\iota$  were mislocalized from the apical membrane and redistributed to the cytoplasm or the basal side of enterocytes in MVID patients. Moreover, Dhekne et al<sup>28</sup> reported that aPKC $\iota$  co-distributes with Rab11a, a MYO5B binding partner, in intestinal epithelial cells. Bryant et al<sup>29</sup> also identified that Cdc42 localized to Rab11a-positive vesicles. These studies provide a potential link between MYO5B, along with its binding partner Rab11a, and polarity complexes comprised of Crumbs3 and Par proteins. As a result, we hypothesized that loss of interaction of MYO5B and Rab11a would result in altered localization of the key apical polarity proteins Crumbs3 and Par complexes.


To dissect the role of Myo5b in regulating polarity complexes, we used germline Myo5b KO mice and intestinal organoids and determined the localization of polarity complexes and tight junction proteins in Myo5b-deficient enterocytes. We observed that Crumbs3 and aPKC co-localize with inclusions as they are forming through apical bulk endocytosis and also are associated with completely internalized inclusions. We further found that inclusions that are contiguous with the apical membrane show an accumulation of Pals1, Patj, Par3, Par6, and the components of the apical junctional complex (claudin-2, zonula occludens [ZO]-1, ZO-2, and occludin) over the top of the inclusion before excision from the brush border. Moreover, we show that a pig model of MVID showed claudin-2 concentrated over inclusions that were forming from the apical membrane. Data acquired from 2 unique animal models of MVID suggested that inclusion formation is accompanied by a concentration of tight junction proteins immediately above forming inclusions. We postulate that this unique accumulation of tight junctional components above the neck of inclusion endocytosis may provide a seal at the site of apical bulk endocytosis in enterocytes.

## Results

### *Loss of Myosin Vb In Vivo Results in Microvilli Lined Inclusions Associated With Rab11a*

Impairment of the molecular motor Myo5b gives rise to numerous cytoplasmic vacuoles, known as *intracellular microvillus inclusions*. This phenomenon has been shown in multiple animal models, including germline Myo5b KO mice,<sup>18,30</sup> a MYO5B gene-edited pig model,<sup>10</sup> and in

**Abbreviations used in this paper:** aPKC, atypical protein kinase C; Cdc42, cell division control protein 42 homolog; DMSO, dimethyl sulfoxide; EPEC, enteropathogenic *Escherichia coli*; ERM, ezrin–radixin–moesin; KO, knockout; MVID, microvillus inclusion disease; MYO5B, myosin Vb; Pals1, proteins associated with Lin-7; Patj, Pals1-associated tight junction protein; PBS, phosphate-buffered saline; P-ERM, phosphorylated ezrin–radixin–moesin; Rab, Ras-related in brain; SEM, scanning electron microscope.

 Most current article

© 2021 The Authors. Published by Elsevier Inc. on behalf of the AGA Institute. This is an open access article under the CC BY-NC-ND license (<http://creativecommons.org/licenses/by-nc-nd/4.0/>).

2352-345X

<https://doi.org/10.1016/j.jcmgh.2021.01.022>

morpholino-depleted zebrafish.<sup>31</sup> We recently showed that inclusions form through a novel process of apical bulk endocytosis.<sup>16</sup> However, the exact mechanisms regulating inclusion formation are incompletely understood and currently understudied. To address these gaps in knowledge, we used germline Myo5b KO mice and systematically compared them with neonatal control (wild-type or heterozygous) littermates that lacked inclusions. In the normal neonatal mouse intestine, the enterocyte brush border is lined by Ezrin, which links apical membrane proteins with the underlying actin cytoskeleton (Figure 1A). Small intestinal enterocytes typically express the cytoskeleton marker  $\gamma$ -actin, which is enriched in the absorptive brush border (Figure 1B). Consistent with previous reports in neonatal control mice, we observed  $\alpha$ -actinin 4 localized to the terminal web and the apical junctional complexes<sup>32,33</sup> (Figure 1B). In contrast, in Myo5b KO mice, inclusions could be visualized in enterocytes along the length of the villi. These inclusions stained for Ezrin and could be seen invaginating from the membrane or within the cytoplasm (Figure 1A). In Myo5b KO mice, intracellular inclusions were lined by microvilli ( $\gamma$ -actin<sup>+</sup>) and surrounded by  $\alpha$ -actinin in enterocytes (Figure 1B), indicating that the terminal web was endocytosed along with the brush border during inclusion formation. Moreover, Myo5b KO enterocytes had less distinct lateral membranes marked by  $\alpha$ -actinin, and cytoplasmic  $\alpha$ -actinin also was observed, suggesting that loss of Myo5b alters  $\alpha$ -actinin localization in enterocytes. These findings support our previous studies suggesting that microvillus inclusions in Myo5b KO mice form through invagination of the apical membrane of enterocytes in a process termed *apical bulk endocytosis*.<sup>16</sup>

Rab11a is a Myo5b binding protein that has been implicated in inclusion formation in MVID.<sup>17,34</sup> To determine whether Rab11a may be involved in inclusion formation, we performed immunofluorescence staining for Rab11a in littermate control and Myo5b KO mice (Figure 1C). The proximal small intestine of control mice showed Rab11a concentrated in the subapical compartment below the apical brush border in enterocytes. In contrast, neonatal Myo5b KO mice showed Rab11a closely associated with numerous inclusions adjacent to the apical brush border and fully internalized. Rab11a accumulated around inclusions in Myo5b KO enterocytes and also was present as puncta in the cytoplasm, providing further evidence that loss of Myo5b in vivo disrupts the normal localization of Rab11a.

To visualize the structure of inclusions during formation, phalloidin staining was performed to label F-actin in frozen sections from littermate neonatal control and Myo5b KO mice. Confocal imaging of the proximal small intestine of mice to acquire z-stack projections showed a well-developed brush border in control mice with no inclusions (Figure 1D). In Myo5b KO mice, numerous inclusions were apparent in z-stack projections, several of which appeared to be excising from the apical membrane. To better visualize the 3-dimensional nature of inclusions, we used scanning electron microscopy (SEM) of fractured duodenal villi from Myo5b KO mice (Figure 1E). SEM images show the formation of inclusions from the apical membrane and highlight the brush border surrounding inclusions.

### *The Par Polarity Complex Is Associated With Inclusions in Myo5b-Deficient Enterocytes*

At present, the role of polarity complexes has not been investigated in animal models of MVID or in the setting of inclusion formation. Past work has suggested that there is endocytic regulation of cellular polarity and that, reciprocally, polarity regulators impact endocytosis. Extensive work in *Caenorhabditis elegans* indicates that polarity modules are required for endocytosis.<sup>35–37</sup> To determine whether polarity complexes were involved in the process of apical bulk endocytosis in Myo5b KO enterocytes, we performed immunostaining for the polarity complexes beginning with the Par polarity complex, composed primarily of aPKC, Par3, and Par6.

Immunofluorescence of neonatal control mouse proximal small intestine showed aPKC enriched at the apical tight junction complex and localized to the apical membrane in the top half of the villi (Figure 2A). In neonatal Myo5b KO mouse small intestine, aPKC was similarly present in the apical junctions and apical membrane, but it also was concentrated in inclusions as identified by  $\gamma$ -actin staining. Par3 immunostaining showed normal localization to the apical junctions in control mice. In contrast, Myo5b KO mice showed increased cytoplasmic staining for Par3 and a close association of Par3 with forming inclusions present at the apical membrane (Figure 2B). The localization of Par6 was similar to that of Par3, with Par6 being evident at the apical tight junctions of enterocytes in control mice (Figure 2C). Par6 was present at the apical junctions of Myo5b KO mouse enterocytes, but also had increased cytoplasmic Par6, and Par6 also localized immediately above inclusions that were contiguous with the brush border. The altered localization of aPKC, Par3, and Par6 suggests that Myo5b regulates the positioning of these polarity complexes in vivo and suggests that the Par complex may be involved in inclusion formation in Myo5b KO mice.

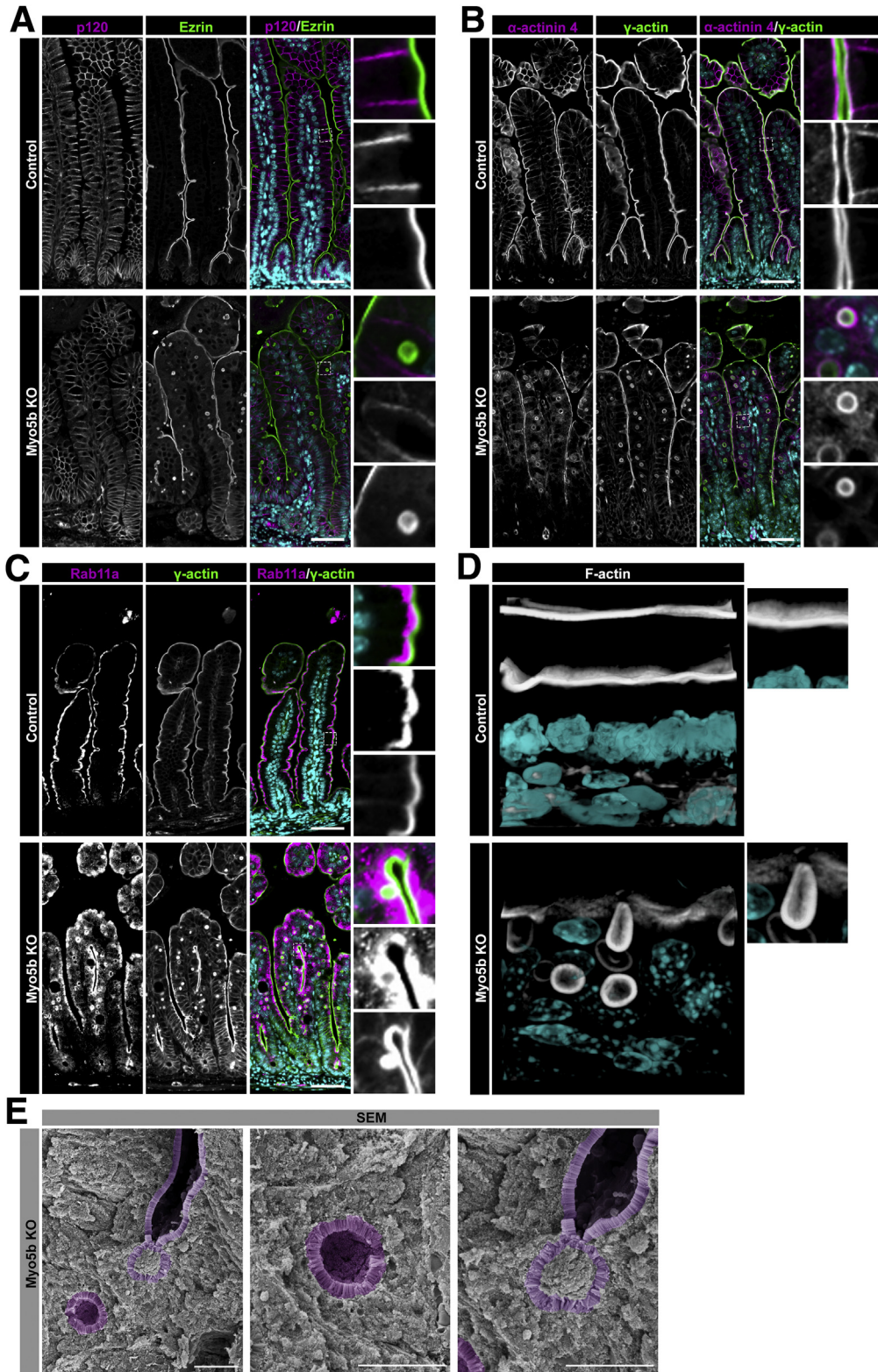
### *Crumbs3 and Its Binding Partner, Pals1, Are Concentrated in Inclusions in Neonatal Myo5b KO Mice*

Next, we sought to examine the other apical polarity complex, Crumbs3, in the setting of Myo5b loss. The Crumbs family of proteins is known to regulate the establishment and maintenance of epithelial cell polarity.<sup>19,20,24,38</sup> Of the 3 mammalian Crumbs isoforms, Crumbs3 is widely expressed in epithelial tissues, including the gastrointestinal tract.<sup>39</sup> Crumbs3 binds ezrin–radixin–moesin (ERM) proteins that link the cell membrane to the underlying actin cytoskeleton in epithelial cells.<sup>19,39–41</sup> To determine whether Crumbs3 localization is altered after loss of Myo5b, we immunostained for Crumbs3 in the proximal small intestine of neonatal control and Myo5b KO mice. In neonatal control mice, Crumbs3 was localized to the apical membrane of enterocytes delineated by phosphorylated ERM (P-ERM) immunofluorescence, as expected and previously reported<sup>19</sup> (Figure 3A). In Myo5b KO mice, Crumbs3 also localized to the apical membrane. However, strong Crumbs3

immunofluorescence was observed near the apical aspect of the lateral membrane and in forming and internalized inclusions as visualized by P-ERM immunostaining. Crumbs3 was concentrated in inclusions both at the membrane and in

fully internalized inclusions within enterocytes in Myo5b KO mice.

Crumbs3 binds Pals1 through its carboxy terminal tail.<sup>42</sup> We predicted that similar to Crumbs3, Pals1 localization



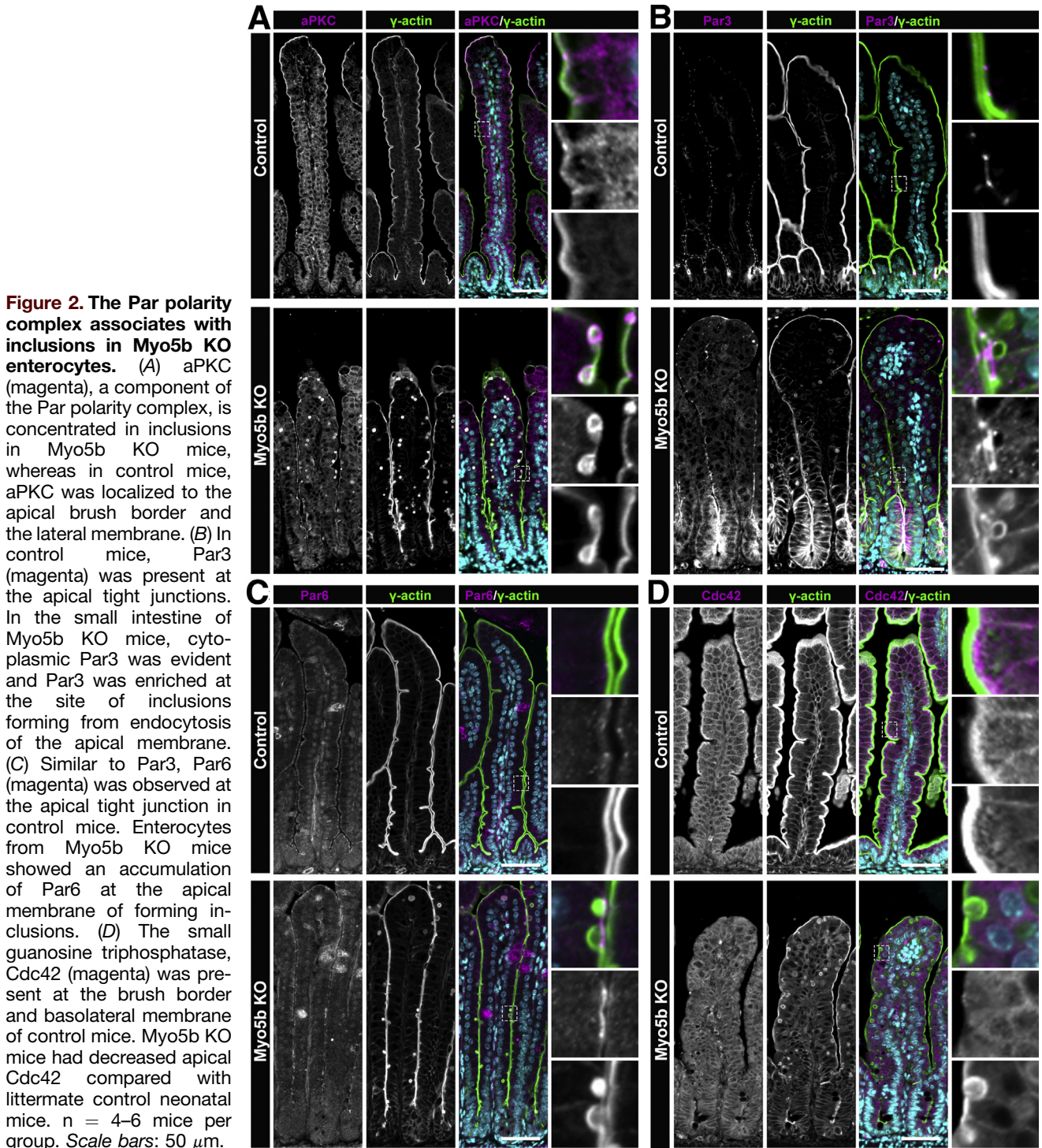


**Figure 1. Myo5b KO mice have microvilli-lined inclusions associated with  $\alpha$ -actinin and Rab11a.** (A) Immunofluorescence staining for the basolateral protein p120 (magenta) and the plasma membrane and actin cytoskeleton linker Ezrin (green) shows the presence of numerous intracellular inclusions in Myo5b KO mice. (B) Micrograph of  $\alpha$ -actinin-4 (magenta), which delineates the terminal web immediately below the apical brush border and the lateral membrane of intestinal epithelial cells and  $\gamma$ -actin (green), which identifies the actin-rich apical membrane immunostaining. No intracellular inclusions were observed in the proximal small intestine of neonatal control mice. Myo5b KO mice had numerous  $\gamma$ -actin-positive inclusions that also were ringed by  $\alpha$ -actinin-4. (C) The small intestine of littermate control and Myo5b KO mice were stained for Rab11a (magenta) and  $\gamma$ -actin (green), which showed altered Rab11a localization in Myo5b-deficient enterocytes. Moreover, Rab11a surrounded numerous inclusions at the apical membrane and inclusions that were fully internalized. (D) Z-stack projections of the proximal small intestine of control and Myo5b KO mice to visualize the 3-dimensional nature of inclusions after loss of Myo5b. (E) Fracture SEM was performed on neonatal small intestine from Myo5b KO mice to view microvilli-lined inclusions. A completely internalized inclusion (pseudocolored magenta) and a forming inclusion (pseudocolored purple) are shown.  $n = 4-6$  mice per group. Scale bars (immunofluorescence images): 50  $\mu\text{m}$ . Scale bars (SEM from left to right): 10  $\mu\text{m}$ , 5  $\mu\text{m}$ , 5  $\mu\text{m}$ .

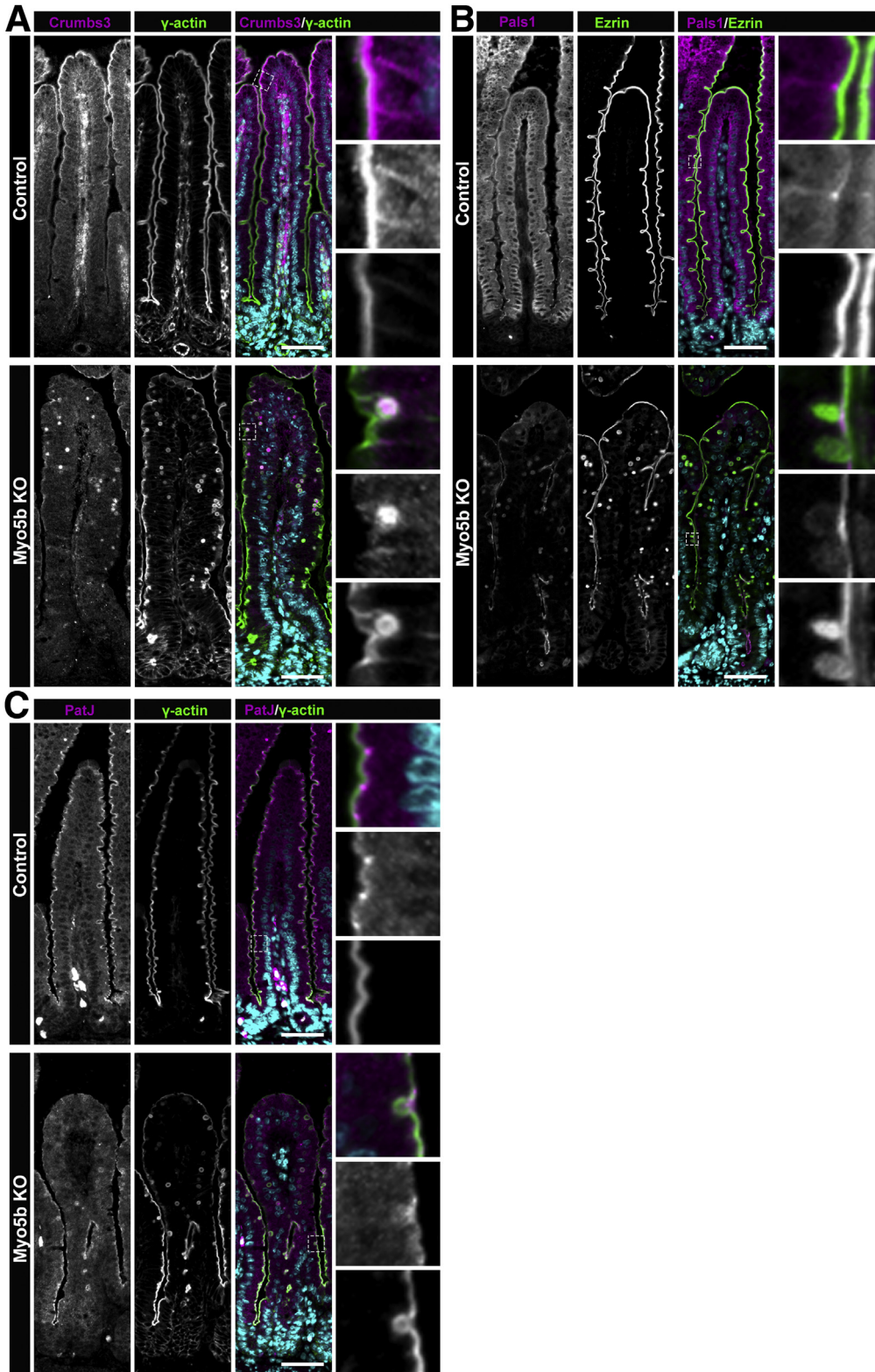


**Figure 3.** Micrographs of components of the Crumbs3 polarity complex in control and Myo5b KO proximal small intestine. (A) Crumbs3 (magenta) and  $\gamma$ -actin (green) staining showed Crumbs3 localized to the apical membrane and lateral membrane in control mice. In Myo5b KO mice Crumbs3 was concentrated in both internalized and forming inclusions. (B) The Crumbs3 binding partner Pals1 (magenta) was present at the apical junctional complex of enterocytes in control mice. In Myo5b KO mice, Pals1 was associated with inclusions. (C) PatJ (magenta), another Crumbs3 polarity complex protein, was localized to the apical junctional complex in the proximal small intestine of control mice. In Myo5b KO mice, PatJ was enriched at the site of inclusions forming from internalization of the apical membrane.  $n = 4-6$  mice per group. Scale bars: 50  $\mu$ m.

also would be impacted by loss of Myo5b in the mammalian small intestine. Immunostaining for Pals1 in the neonatal proximal small intestine showed that Pals1 was localized primarily to the apical membrane with enrichment of Pals1 near the apical junctional complex (Figure 3B). Similar to

our controls, apical Pals1 localization was observed in Myo5b KO mice. However, consistent with our observations for Crumb3, Pals1 also was present in inclusions identified by  $\gamma$ -actin immunostaining. In Myo5b KO enterocytes, Pals1 was concentrated at the apical membrane, where inclusions

were forming through endocytosis. The enrichment of Pals1 in forming inclusions and inclusions that are fully internalized suggests that Crumbs3 and Pals1 are involved in inclusion formation after loss of Myo5b.

Pals1 can bind Patj, acting as an adaptor mediating Crumbs3 and Patj interaction indirectly and forming the Crumbs3/Pals1/Patj polarity complex.<sup>43</sup> Patj is postulated to stabilize the Crumbs3 complex,<sup>44</sup> so we next sought to determine whether the localization of Patj was altered by loss of Myo5b in vivo in mammalian small intestine. In the small intestine of neonatal control mice, Patj was localized immediately below the brush border and was concentrated around apical junctions, closely coinciding with other reports in mammalian cell lines (Figure 3C).<sup>45–48</sup> In Myo5b KO mice, the apical localization of Patj was less evident, especially in the top half of villi. Furthermore, Patj was concentrated around inclusions and at the apex of inclusions contiguous with the apical membrane. Inclusions that had not excised from the apical membrane had an accumulation of Patj, suggesting that Patj may play a role in the complete internalization of inclusions in enterocytes of Myo5b KO mice.

### *The Localization of Tight Junction Proteins Is Altered in Myo5b KO Enterocytes*

Crumbs3 can regulate tight junction formation in mammalian cells through its binding partners including Pals1 and Patj.<sup>43,47,49,50</sup> In particular, Patj associates with many tight junction scaffolding proteins including ZO proteins.<sup>47</sup> Therefore, we next sought to determine whether Myo5b KO mice had altered tight junction protein localization in the small intestine. Claudin-2 is a paracellular cation-selective channel that is expressed and located at the tight junction in neonatal small intestinal villi.<sup>51</sup> As expected, immunostaining for Claudin-2 in neonatal control mice showed normal localization, with Claudin-2 appearing near the apical-most edge of lateral membranes in the apical junction complex of enterocytes along the villi<sup>52</sup> (Figure 4A). In contrast, neonatal Myo5b KO mice showed aberrant Claudin-2 localization in enterocytes emerging from the crypts. At the base of the villi, Claudin-2 was located intracellularly inside of Myo5b KO enterocytes. Enterocytes located in the top two thirds of the villi showed more regular distribution of Claudin-2. However, Claudin-2 was highly concentrated at the apical membrane of enterocytes where inclusions were forming from endocytosis of the apical membrane along the length of villi. Inclusions that were contiguous with the apical membrane showed a dense accumulation of Claudin-2 immediately above the inclusion.

To determine whether other tight junction proteins are associated with inclusion formation similarly to claudin-2, we immunostained for ZO-1, ZO-2, and occludin in neonatal control and Myo5b KO mice. ZO-1, ZO-2, and occludin were distributed normally in the apical junctional complexes in the proximal small intestine of control mice (Figure 4B–D). Similar to claudin-2, Myo5b KO mice showed discrete accumulation of ZO-1, ZO-2, and occludin at the

apical membrane above inclusions that were forming through endocytosis of the brush border in enterocytes.

To determine whether tight junction proteins remained attached to inclusions after excision from the apical membrane and internalization, we focused on cytoplasmic inclusions in Myo5b KO mice. We observed that occasionally subapical inclusions were associated with claudin-2 staining (Figure 5A). Immunostaining for ZO-1 (Figure 5B), ZO-2 (Figure 5C), and occludin (Figure 5D) showed that internalized inclusions were rarely positive for tight junction proteins. These data suggest that during inclusion excision, ZO-1, ZO-2, and occludin remain at the apical membrane and are not internalized or excised from the apical membrane. The enrichment of tight junction proteins at the apical membrane of enterocytes during inclusion formation suggests that tight junction components are either being recruited to the apical membrane or are being inserted at the site of inclusion formation *de novo*. These data suggest a unique role for tight junction proteins in inclusion formation and internalization.

### *ZO-1 and Claudin-2 Accumulate Over Forming Inclusions in Myo5b KO Mice*

To better visualize the apical accumulation of tight junction components during inclusion formation in Myo5b-deficient enterocytes, we used confocal microscopy to generate 3-dimensional z-stack projections (Figure 6A). Frozen sections (25  $\mu$ m) were immunostained for claudin-2, and phalloidin was used to label F-actin to delineate the apical brush border and inclusions (Figure 6A). In the z-stack projection, inclusions that are forming from apical bulk endocytosis appear to have a dense accumulation of claudin-2 immediately above the forming inclusion. This cap or patch of claudin-2 lacks F-actin. Immunostaining for ZO-1 showed a similar pattern of accumulation over the site of inclusion formation (Figure 6B). These observations suggest that claudin-2 and ZO-1 may be accumulating over the inclusions, perhaps to act as a seal as the inclusion is excised from the apical membrane. Indeed, the grayscale images of claudin-2 and ZO-1 both appear to show tight junctions feeding into the dense cap or patch over the inclusion.

We next quantified the number of inclusions that still were attached to the apical membrane and were associated with apical accumulation of tight junction proteins claudin-2 or ZO-1 immediately above inclusions (Figure 6B). As expected, no inclusions were observed in neonatal control mice. In Myo5b KO mice, approximately 47% of inclusions that were contiguous with the apical membrane had claudin-2 present at the apical membrane of the forming inclusion. Quantification of forming inclusions that also had an accumulation of apical ZO-1 in Myo5b KO mice showed that approximately 80% of forming inclusions also were positive for ZO-1. These data suggest that recruitment of tight junction proteins during apical bulk endocytosis to form inclusions in Myo5b-deficient enterocytes occurs in a large majority of forming inclusions.

To determine whether inclusion formation in the setting of MVID may be forming similarly to inclusions in Myo5b KO

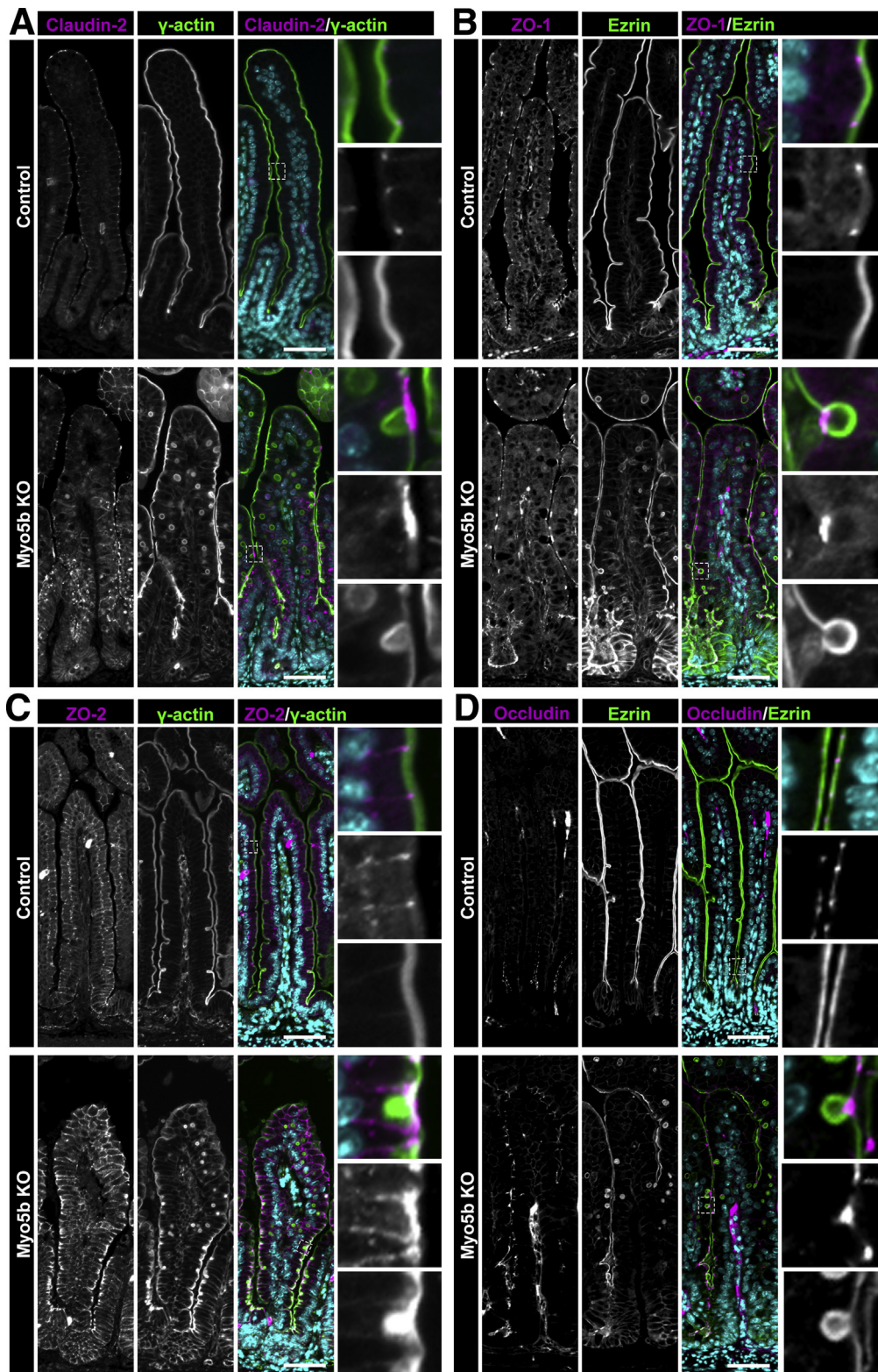


**Figure 4. Apical tight junction proteins accumulate at the sites of inclusion formation in Myo5b KO enterocytes.** In control mice, the apical tight junction proteins (A) claudin-2, (B) ZO-1, (C) ZO-2, and (D) occludin (all in magenta) were distributed normally at the site of apical cell-cell contact in control mice. (A) In Myo5b KO mice, claudin-2 was found to be dispersed within the cytoplasm in enterocytes at the base of the villi and was associated with inclusions at the apical membrane. (B) ZO-1, (C) ZO-2, and (D) occludin also accumulated at the site of brush-border endocytosis of forming inclusions in Myo5b-deficient enterocytes.  $n = 4-6$  mice per group. Scale bars: 50  $\mu\text{m}$ .

mice, we used small intestinal tissue from pigs that were genetically edited to express a homolog of a mutation in Myo5b that results in MVID in patients in the Navajo Nation. Patients with MVID cannot tolerate enteral feeding, have villous atrophy, and are reported to have inclusions in

approximately 10%–20% of enterocytes.<sup>15</sup> Thus, intestinal specimens from MVID patients rarely have discernible inclusions forming from the apical membrane that are well oriented with good cellular architecture and morphology. Therefore, we examined tissue from a pig model of MVID



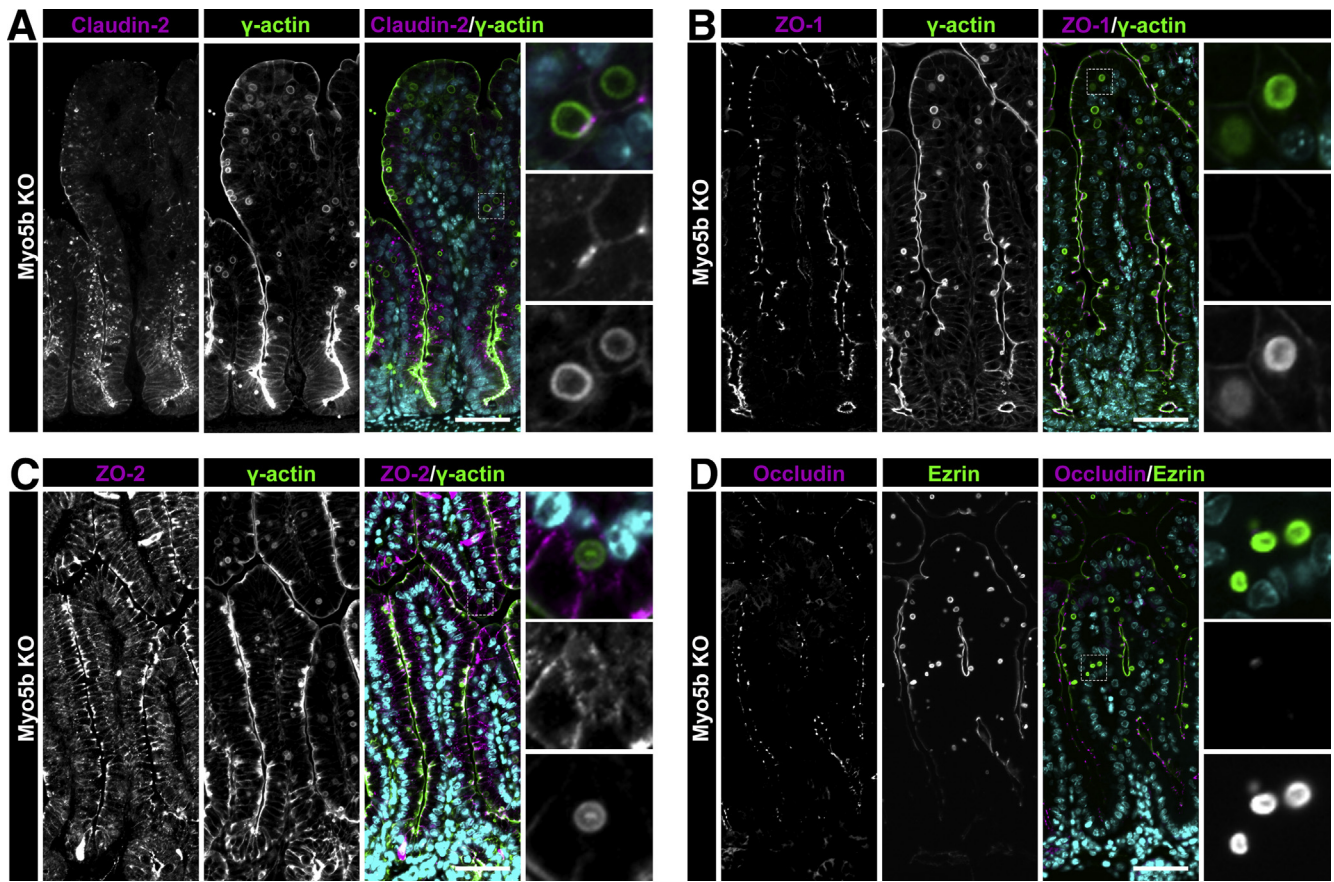


**Figure 5. Cytoplasmic inclusions lack ZO-1, ZO-2, and occludin, and infrequently associate with claudin-2.** (A) Immunostaining for tight junction proteins in Myo5b KO mice showed internalized inclusions occasionally stained positive for claudin-2. In Myo5b KO, small intestine inclusions rarely contained (B) ZO-1, (C) ZO-2, or (D) occludin.  $n = 4-6$  mice per group. Scale bars: 50  $\mu\text{m}$ .

that closely recapitulates the human MVID phenotype, including the presence of inclusions throughout the small intestine.<sup>10</sup> Immunostaining for claudin-2 and  $\gamma$ -actin showed the presence of claudin-2 above inclusions that appear to be contiguous with the apical membrane (Figure 7A). The presence of claudin-2 over inclusions forming through endocytosis in the pig model of MVID suggests that tight junction proteins likely are involved in inclusion formation in patients with MVID.

### Cortactin Localization During Apical Bulk Endocytosis

Cortactin is an actin binding protein that is recruited to sites of endocytosis.<sup>53-55</sup> To determine whether cortactin was localized to sites of apical bulk endocytosis, we immunostained for cortactin, ZO-1, and P-ERM in neonatal control and Myo5b KO mice (Figure 8). In the small intestine of control mice, cortactin was observed to localize immediately below the apical membrane and at the tight junction where the signal overlapped with ZO-1 (Figure 8A), consistent with previous reports.<sup>56,57</sup> In Myo5b KO mice, cortactin was observed at the site of inclusion formation and was found to co-localize with ZO-1. Maximum-intensity Z-

stack projections of Myo5b KO tissue showed inclusions at the membrane with discrete cortactin puncta associated with ZO-1 caps (Figure 8B). Thus, we hypothesize that tight junctions orchestrate the molecular machinery to facilitate inclusion scission through cortactin. Based on literature that shows a link between ZO-1, cortactin, and dynamin,<sup>56,58-62</sup> we propose that membrane perturbation caused by apical bulk endocytosis recruits tight junction proteins to form a cap over the forming inclusion/bulk endosome. Because ZO-1 interacts with cortactin and cortactin links the actin cytoskeleton and dynamin (including dynamin 2),<sup>53,58,61,63</sup> we speculate that as the ZO-1 cap forms, cortactin directs dynamin to the neck of the forming bulk endosome to enable scission of the inclusion from the apical membrane.

### Inclusion Formation in Small Intestinal Organoids Derived From Myo5b KO Mice Is Independent of aPKC Activity

The generation of small intestinal organoids allows for the long-term propagation of progenitor cells from intestinal stem cells, which can be differentiated to form multiple cellular lineages in vitro that recapitulate the native small

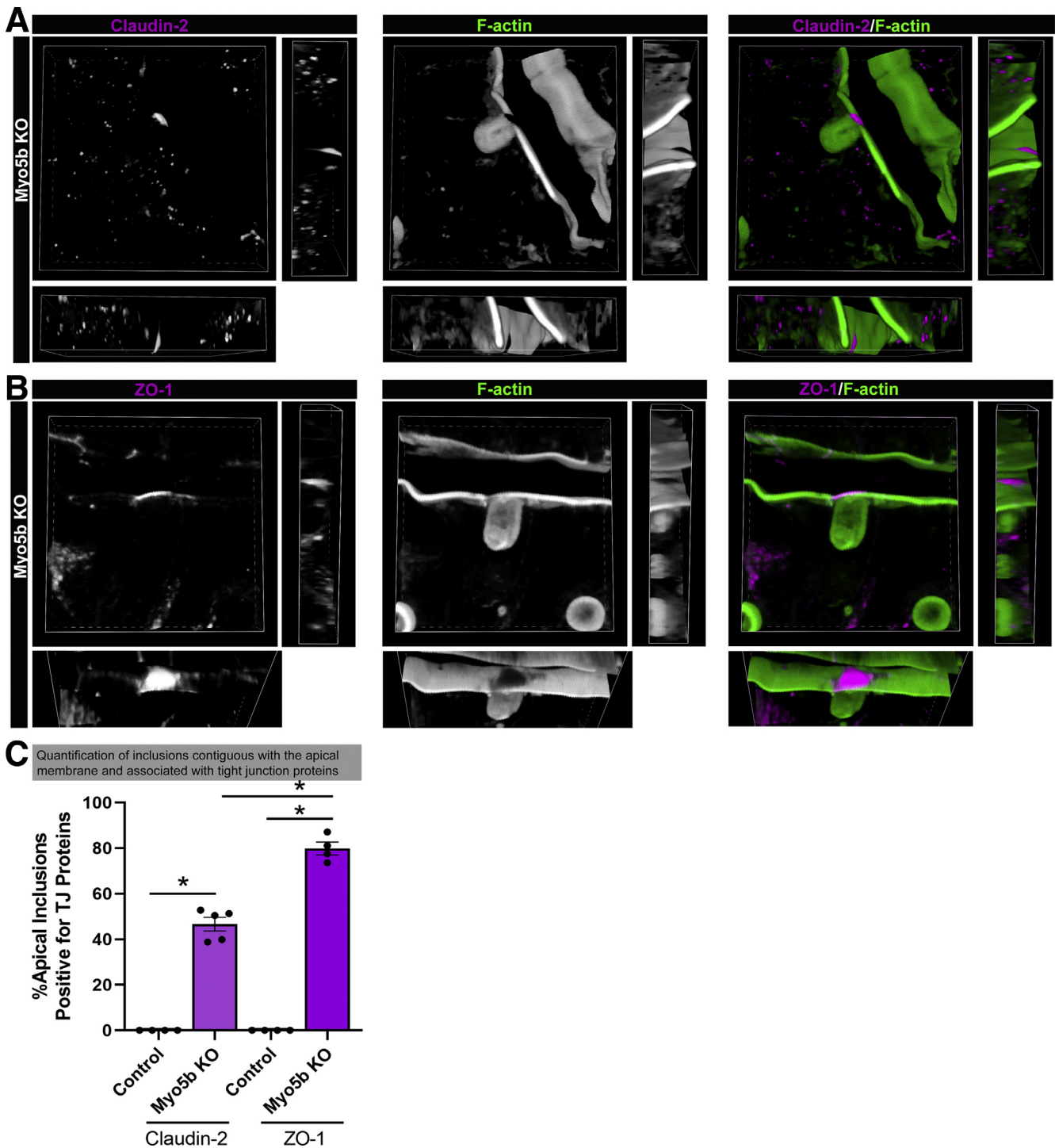


**Figure 6. Three-dimensional imaging of inclusions in Myo5b KO proximal small intestine show a cap of claudin-2 and ZO-1 formed over inclusions contiguous with the apical membrane.** Imaging of 25- $\mu$ m frozen sections of Myo5b KO proximal small intestine showed the dense accumulation of (A) claudin-2 (magenta) and (B) ZO-1 (magenta) immediately above forming inclusions identified by F-actin (green). Claudin-2 and ZO-1 appear to form a cap over inclusions where F-actin is absent. (C) Quantification of total inclusions that were present at the apical membrane and inclusions that were contiguous with the apical membrane and positive for Claudin-2 or ZO-1. \* $P < .05$ ,  $n = 4-5$  mice per group. TJ, tight junction.

intestinal milieu.<sup>64</sup> We used the organoid culture system to determine whether inclusion formation in vitro was dependent on aPKC. Myo5b KO organoids were treated with dimethyl sulfoxide (DMSO) vehicle or 10  $\mu$ mol/L  $\zeta$ -Stat, an

aPKC inhibitor. Two days after crypt isolation and organoid formation, intestinal organoids were differentiated and DMSO or 10  $\mu$ mol/L  $\zeta$ -Stat was administered during differentiation. Intestinal organoids require differentiation to

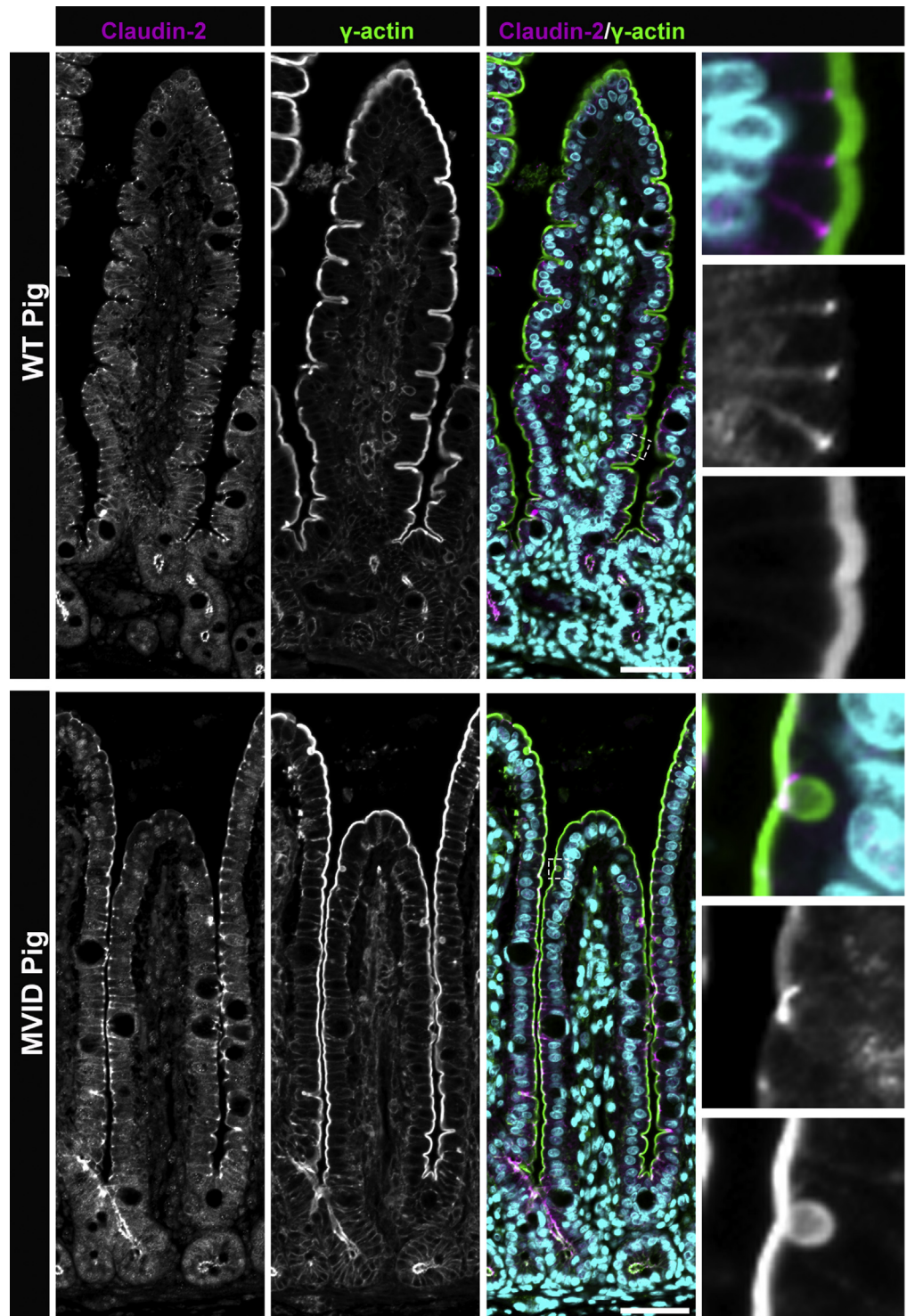


**Figure 7. Inclusions at the apical membrane have enrichment of claudin-2 in a pig model of MVID.** Small intestinal tissue from aged matched wild-type (WT) pigs and pigs that expressed a P663L mutation in MYO5B that resulted in MVID were immunostained for claudin-2 (magenta) and  $\gamma$ -actin (green) to determine whether a physiologically relevant model of MVID formed inclusions in a similar manner as Myo5b KO mice. Inclusions in MVID pigs showed claudin-2 accumulated at the site of inclusion formation.  $n = 2$  MVID pigs and 3 WT pigs. Scale bars: 50  $\mu$ m.

develop robust inclusion formation.<sup>16,65</sup> Inclusion formation in DMSO and  $\zeta$ -Stat treatment resulted in a similar number of inclusions identified by F-actin staining (Figure 9A). Therefore, treatment of Myo5b KO intestinal organoids with  $\zeta$ -Stat did not prevent inclusion formation, suggesting that inclusion formation is not entirely dependent on aPKC or

that there are redundancies in the functions of polarity proteins. Immunostaining of Myo5b KO intestinal organoids for Crumbs3 showed no alteration in Crumbs3 after inhibition of aPKC (Figure 8B). However, Crumbs3 intensity was decreased in Myo5b KO intestinal organoids treated with  $\zeta$ -Stat compared with DMSO-treated organoids.

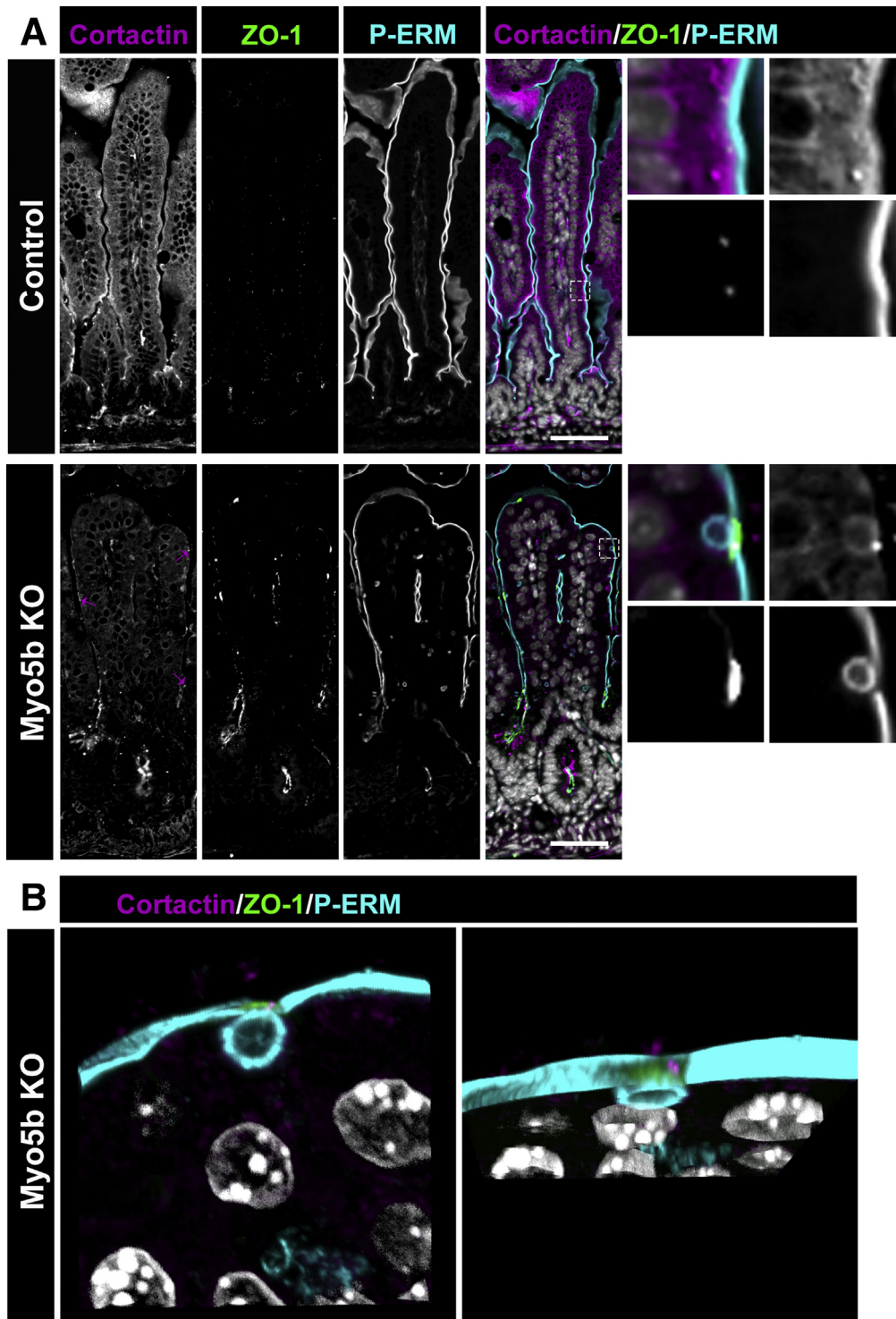


**Figure 8.** Cortactin associates with ZO-1 during inclusion formation in Myo5b KO mice. (A) Immunostaining for cortactin (magenta), ZO-1 (green), P-ERM (cyan), and nuclei (white) in control and Myo5b KO mice. Magenta arrows indicate cortactin at sites of inclusion formation in Myo5b KO mice. (B) Maximum-intensity Z-stack projection of a representative inclusion in a Myo5b KO enterocyte.  $n = 4$  mice per group. Scale bars: 50  $\mu\text{m}$ .

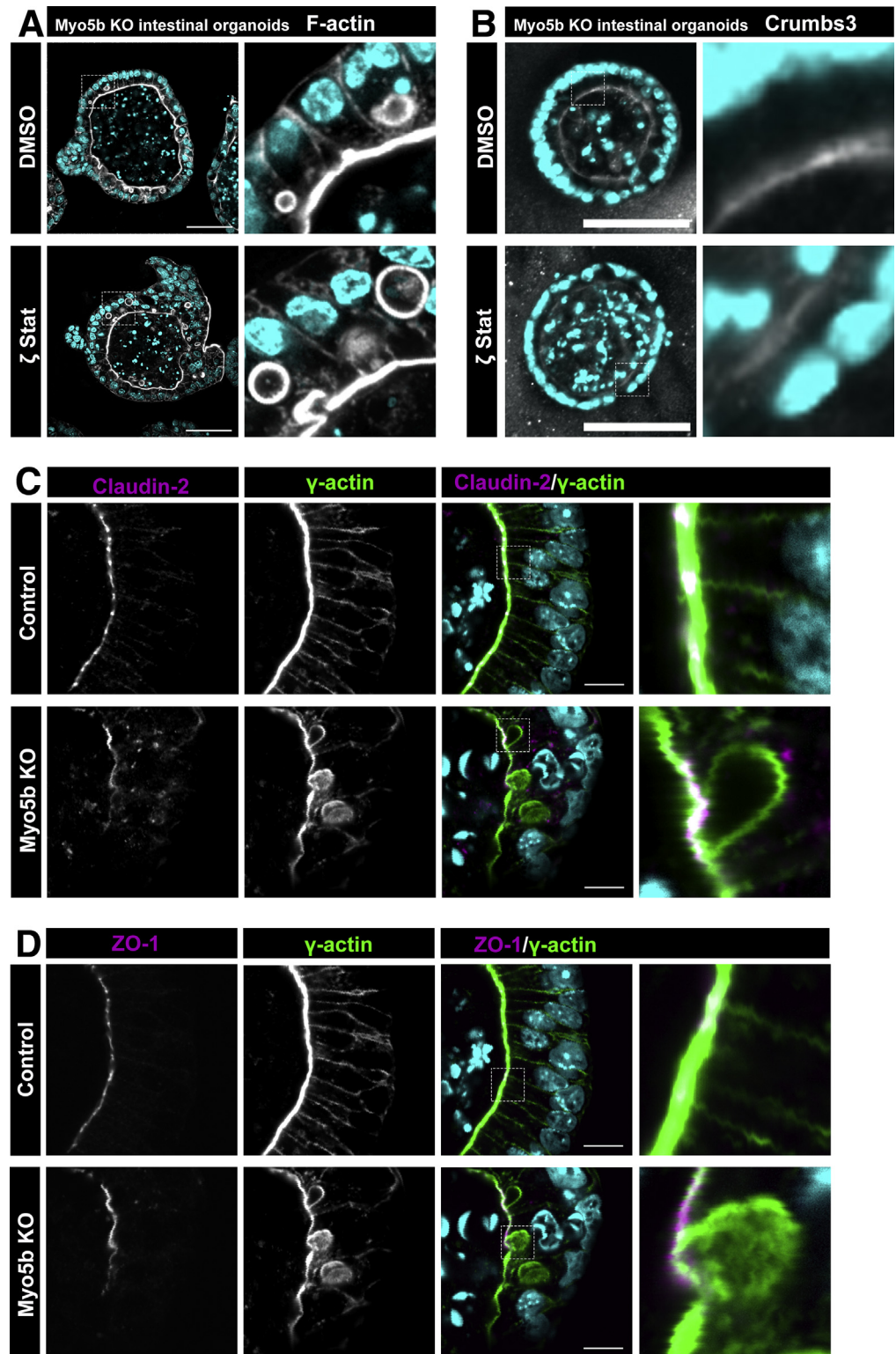
Immunostaining for ZO-1 and claudin-2 in organoids generated from control and Myo5b KO showed normal localization at the apical junctional complex in control-derived organoids (Figure 9C and D). In Myo5b KO-derived organoids, claudin-2 was observed at the apical membrane of forming inclusions similar to our observations in the small intestine (Figure 9C). Immunofluorescence for ZO-1 in Myo5b KO organoids showed ZO-1 at the top of the forming inclusion (Figure 9D). These findings suggest that

in vitro inclusion formation in Myo5b KO mice involves recruitment of tight junction proteins likely to promote excision of inclusions before internalization.

## Discussion

In this study, we identified that loss of Myo5b alters the localization of polarity complex proteins Par3, Par6, aPKC, Cdc42, Crumbs3, Pals1, and Patj; MYO5B binding partner

**Figure 9. Intestinal organoids generated from Myo5b KO mice have inclusions that are associated with claudin-2 and ZO-1.** (A) Intestinal organoids derived from the proximal small intestine of Myo5b KO mice were treated with DMSO vehicle or  $\zeta$ -Stat, an aPKC inhibitor to determine whether inhibition of aPKC would prevent inclusion formation. Both DMSO- and  $\zeta$ -Stat-treated intestinal organoids from Myo5b KO mice developed numerous inclusions. (B) Immunostaining for Crumbs3 in DMSO- and  $\zeta$ -Stat-treated Myo5b KO intestinal organoids showed no alteration in the localization of Crumbs3. However, a decreased intensity of Crumbs3 in intestinal organoids treated with  $\zeta$ -Stat was observed compared with DMSO-treated organoids. Intestinal organoids from littermate control and Myo5b KO mice were immunostained for  $\gamma$ -actin and (C) claudin-2 (magenta) or (D) ZO-1 (green). Control-derived organoids showed a normal distribution of claudin-2 and ZO-1, while Myo5b KO mouse-derived organoids showed inclusions that were associated with accumulations of claudin-2 and ZO-1.  $n = 3$  mice per group were used to generate organoids. Scale bars: (C and D) 10  $\mu$ m, and (A and B) 50  $\mu$ m.



Rab11a; and tight junction components claudin-2, ZO-1, ZO-2, and occludin in the small intestine. Our findings provide direct evidence that Myo5b deficiency alters the localization of multiple polarity complexes. Interestingly, these proteins accumulated in or at the site of inclusion formation, suggesting that they play a role in apical bulk endocytosis. We

previously showed that apical bulk endocytosis mirrors neuronal activity-dependent bulk endocytosis requiring Pacsin2 and dynamin2 for inclusion formation.<sup>16</sup> The work presented here indicates that endocytic trafficking and polarity complexes are closely associated with the formation of inclusions via bulk endocytosis. Based on our findings, we

postulate that MYO5B regulates multiple aspects of epithelial homeostasis, including cell polarity, tight junction protein distribution, and localization of ion transporters.

The maintenance of apical-basal polarity and tight junctions that provide cell-cell contact and barrier function in the intestine is required to maintain mucosal integrity. Consistent with the important role of polarity in health, numerous disorders result when polarity is perturbed. These pathologies include MVID,<sup>5,66</sup> diarrhea resulting from enteropathogenic *Escherichia coli* (EPEC) infection,<sup>67-69</sup> inflammatory bowel disease,<sup>70,71</sup> celiac disease,<sup>72</sup> and cancer.<sup>73</sup> Two studies recently reported decreased expression of MYO5B in gastric cancer<sup>74,75</sup> and 1 study has implicated loss of MYO5B in colorectal cancer.<sup>76</sup> Because loss of polarity is an early event in epithelial cancers, decreased expression of MYO5B may be a precursor to perturbation of polarity complexes and the onset of intestinal epithelial cancers. These studies and our work suggest an interaction between MYO5B and polarity complexes.

Microvillus inclusions are formed over 3-4 hours through a novel mechanism of apical bulk endocytosis, which requires both Pacsin2 and dynamin2.<sup>16</sup> This mechanism in enterocytes has overlapping characteristics with activity-dependent bulk endocytosis described during neuronal hyperstimulation.<sup>77-81</sup> The accumulation of tight junction proteins (claudin-2, ZO-1, ZO-2, and occludin) at the site of inclusion formation suggests that tight junction proteins may be recruited to sites of apical bulk endocytosis to promote excision and internalization within Myo5b KO enterocytes. Studies with EPEC have shown tight junction recruitment at the site of pedestal formation. EPEC induces actin-rich pedestal formation in intestinal epithelial cells and disrupts Par polarity complexes perturbing tight junctions.<sup>82-86</sup> The *E coli* effector EspF is injected into host cells and recruits junctional scaffold proteins ZO-1 and ZO-2 into the actin-rich pedestal during infection.<sup>86</sup> Moreover, tight junction components were found to co-localize with the actin-rich pedestals. Notably, claudin-1 was found at the tip of the pedestal immediately below the bacteria after *E coli* infection of rabbit kidney 13 (RK13) cells.<sup>86</sup> Tapia et al<sup>82</sup> recently showed that EPEC recruits active aPKC to actin within pedestals and away from polarity complexes. They suggested that EPEC-induced recruitment of active aPKC may be the initiating event that leads to disrupted tight junctions. These findings coincide with our data, which show aPKC concentrated in inclusions in Myo5b KO mice. The accumulation of aPKC in forming inclusions may recruit tight junction proteins from the apical junctional complex as well as polarity complex proteins to the site of inclusion formation in Myo5b-deficient enterocytes.

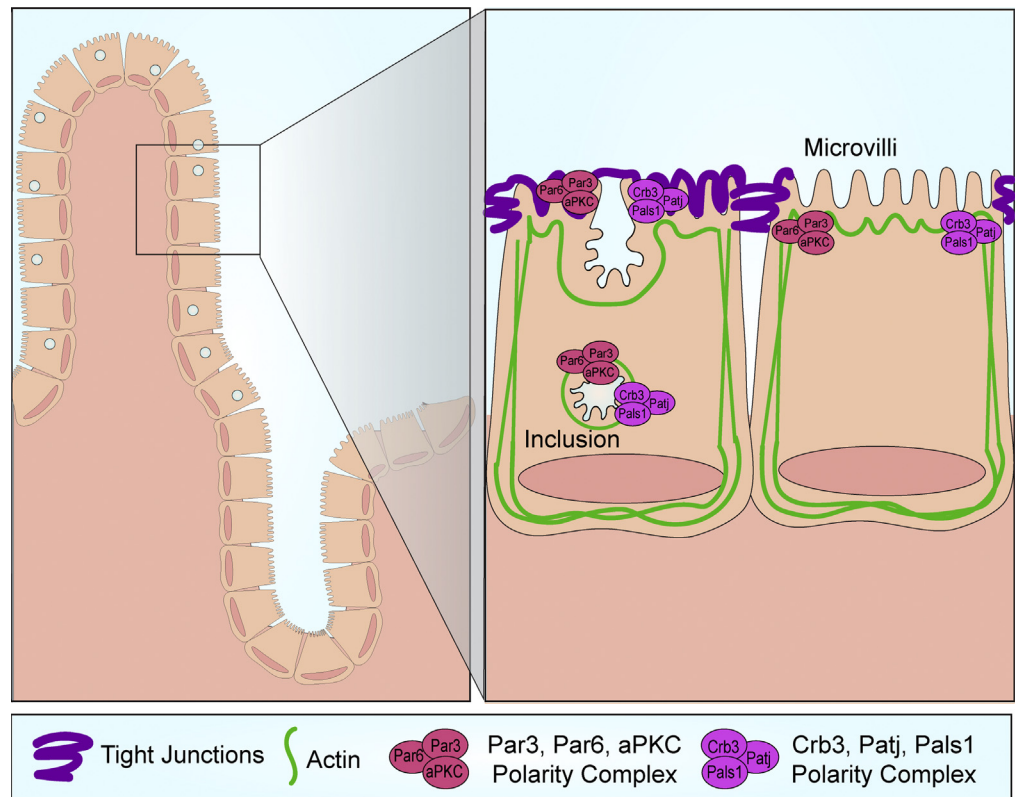
The presence of intracellular inclusions lined by microvilli is not unique to loss of Myo5b. Indeed, numerous knockout mouse models have shown the presence of apical membrane components intracellularly, including for Rab8a,<sup>87</sup> Rab11a,<sup>88</sup> Rab8a;Rab11a double KO,<sup>89</sup> Cdc42,<sup>90,91</sup> and endotubulin.<sup>92</sup> Intracellular inclusions in various genetic mouse models suggest overlapping pathways, which likely all involve altered expression of polarity proteins. To date, all mouse models that show inclusions in the small intestine

enterocytes show the hallmarks of dysregulated polarity. For example, Cdc42-deficient mice have defective polarity and altered junctional protein expression in enterocytes.<sup>91</sup> Rab8a;Rab11a double-knockout mice had mislocalization of PKC $\zeta$  and diminished apical PKC $\zeta$ , again suggesting a polarity defect.<sup>89</sup> Endotubulin interacts with tight junction proteins and regulates the assembly and maintenance of tight junctions, which indicates that it may be associated with other polarity proteins that are found at the apical junctional complex.<sup>93,94</sup> In 3-dimensional Madin-Darby canine kidney (MDCK) cysts, Rab11a and Rab8a were required for the apical localization of Par proteins and Cdc42 to the forming lumen.<sup>29</sup> The presence of inclusions in the small intestine of various genetic mouse models points to the critical roles of polarity complexes in inclusion formation. Our study extends these findings by specifically identifying polarity complexes and tight junction proteins in inclusion formation in Myo5b-deficient mice.

One interesting observation in our study was that inhibition of aPKC in intestinal organoids from Myo5b KO mice did not prevent or diminish inclusion formation. Although aPKC is a member of the Par complex, we speculate that other proteins can compensate in the setting of diminished aPKC activity. This is consistent with previous investigations that have identified redundancy in polarity complexes. To prevent the formation of inclusions in Myo5b KO enterocytes, multiple polarity proteins may need to be knocked out or inhibited. Our findings that aPKC inhibition does not impact inclusion formation support previous data that showed overlapping functions for the apical polarity complexes. For example, Crumbs3 KO mouse embryos show altered intestinal architecture including fused villi,<sup>19,20</sup> however, barrier function and tight junctions were unaffected.<sup>19</sup> This in vivo finding was surprising because work in MCF10a breast epithelial cells showed tight junction formation in response to exogenous Crumbs3, leading Fogg et al<sup>49</sup> to suggest that Crumbs3 regulates tight junction formation. Based on these studies, it is likely that in vivo, multiple polarity proteins or complexes compensate and maintain tight junction formation. In support of this concept, adult inducible VillinCre<sup>ERT2</sup>;Myo5b<sup>flox/flox</sup> mice show many intestinal alterations after loss of Myo5b including diarrhea, however, they do not have an intestinal barrier defect based on tissue resistance and dextran permeability measurements.<sup>11,12</sup>

We observed that in Myo5b KO mice, polarity complex proteins Crumbs3, Patj, Pals1, and aPKC all were present in intracellular inclusions. These findings appear to mirror observations with enteric pathogens. Infection with EPEC results in loss of apical-basal polarity through the EPEC effectors EspF and Map.<sup>95</sup> Tapia et al<sup>95</sup> showed that EspF and Map promote endocytosis of Crumbs polarity proteins (Crumbs3 and Pals1) in intestinal cells, leading to disruption in tight junction proteins and perturbation of polarity. EPEC and *Citrobacter rodentium* both were found to redistribute the Crumbs3 complex from the apical membrane to the cytoplasm of mouse intestinal colonocytes.<sup>95</sup> These data support our findings that polarity complexes and tight junctions are intricately connected. In addition to infection

**Figure 10. Diagram of proposed model of inclusion formation in Myo5b KO enterocytes.** Based on our findings, we propose that during apical bulk endocytosis, tight junction proteins are recruited to cover the forming bulk endosome/inclusion. These tight junction proteins form a dense cap over inclusions that are contiguous with the apical membrane, implying a functional role during apical bulk endocytosis excision from the membrane. In addition, apical polarity complexes (the Crumbs and Par complexes) are present at the apical membrane and in internalized inclusions.



models, knockdown of Patj in human intestinal cells in vitro disrupted the normal apical localization of Crumbs3, resulting in Crumbs3 being present in a large vesicular compartment below the apical membrane.<sup>44</sup> These results mirror our work with microvillus inclusions.

Finally, loss of Cdc42 function increases the endocytic uptake of apical proteins, including Crumbs in *Drosophila*.<sup>96</sup> In *Drosophila*, loss-of-function mutations in aPKC also results in internalization of Crumbs into endosomes.<sup>96,97</sup> Work in *Drosophila* follicle cells and embryos show that Rab11 is essential for Crumbs to maintain its polarized location at the plasma membrane.<sup>97,98</sup> Our results are reminiscent of these findings and suggest that Crumbs3 may be involved in apical bulk endocytosis in Myo5b KO enterocytes. We further speculate that Myo5b may be responsible for the stabilization of the Crumbs3 polarity complex through its binding partner Rab11a.

Although we speculate that polarity complexes are functionally involved in inclusion formation, it also is possible that polarity complexes could be pulled into inclusions simply by association with the actin cytoskeleton through cross-linking proteins. The Crumbs complex interacts with ERM proteins, which couples the cell membrane to the underlying actin cytoskeleton.<sup>19,39,99,100</sup> Pals1 also can bind Ezrin in the stomach and regulates the localization of ezrin in parietal cells.<sup>101</sup> Thus, it is feasible that apical polarity complexes are internalized with inclusions as a result of association with Ezrin. Future work is required to understand the sequence of events that occur during inclusion formation and to determine the specific role of polarity proteins in apical bulk endocytosis.

Figure 10 presents a proposed model of our findings. Loss of Myo5b results in apical bulk endocytosis in small intestinal enterocytes. We postulate that during apical bulk endocytosis tight junction proteins are recruited from surrounding apical junctions to cover the forming bulk endosome/inclusion. These tight junction proteins form a dense cap over inclusions that are attached to the apical membrane. We suggest that this re-localization of tight junction proteins is similar to events that occur in the small intestine in response to cell shedding. By using live imaging of mice expressing fluorescence ZO-1, Guan et al<sup>102</sup> showed that apical ZO-1 redistributes during cell shedding. After a cell is extruded from the epithelium into the intestinal lumen, a gap exists where the cell previously resided, ZO-1 appears to condense and cover this gap.<sup>102</sup> We propose that claudin-2, ZO-1, ZO-2, and occludin redistribute and condense to form a patch over inclusions during apical bulk endocytosis. In addition, during apical bulk endocytosis, apical polarity complexes (the Crumbs and Par complexes) are present at the apical membrane and relocated into internalized inclusions, suggesting that these polarity proteins are involved in inclusion formation.

In summary, this study shows that loss of Myo5b results in the redistribution of the Crumbs3 and Par polarity complexes and the accumulation of tight junction proteins at the site of inclusion formation. Collectively, these data support the conclusion that in vivo loss of Myo5b results in aberrant localization of Rab11a, which likely impacts the normal distribution of polarity complexes including Cdc42. Thus, Myo5b acts to regulate polarity complexes in normal intestinal epithelial cells. Loss of Myo5b induces inclusion formation, in

part through recruitment of tight junction proteins to the sites of apical bulk endocytosis. These findings could have a broad impact, supporting a role for MYO5B in numerous disorders involving alterations in polarity.

## Materials and Methods

### *Animals and Tissue Processing*

Animal care, maintenance, and experimental procedures all were performed with approval from the Institutional Animal Care and Use Committee of Vanderbilt University Medical Center. Germline Myo5b KO mice were generated and characterized for epithelial abnormalities as previously described.<sup>18</sup> Briefly, 2- to 6-day-old mice were killed and the proximal small intestine was excised and fixed for analysis. Littermates, either wild type or heterozygous for Myo5b, were used as controls for all experiments. Myo5b KO mice die approximately 5–7 days after birth from an inability to absorb and retain water.<sup>18</sup> Thus, all mice used in this study were neonatal (age, 2–6 d), including control littermates. The proximal small intestine consisting of the duodenum and jejunum were excised from neonatal mice, washed in phosphate-buffered saline (PBS), and then fixed in either 4% paraformaldehyde (J19943; Thermo Fisher Scientific, Waltham, MA), 10% neutral buffered formalin (16004-128; VWR, Radnor, PA), or 3% glyoxal<sup>103</sup> overnight at 4°C. Fixed tissue was washed in PBS, processed, and embedded in paraffin. For frozen embedding, fixed tissues were washed in PBS, then moved to 30% sucrose in PBS solution and stored overnight at 4°C. After sucrose infiltration, the tissues were embedded in optimal cutting temperature compound (4583; Sakura, Torrance, CA) and frozen at -80°C. Thick frozen sections (25 μm) were cut using a cryostat and sections were used for immunostaining. The gene editing and generation of a pig model of MVID, as well as a detailed harvesting protocol, was described previously.<sup>10</sup> Briefly, swine primary fetal fibroblasts were edited with transcription activator-like effector nucleases and homology-directed repair oligonucleotide template containing the P663L mutation of the MYO5B gene, which then were cloned via somatic cell nuclear transfer. Small intestinal tissues from wild-type and MVID (MYO5B[P663L]) piglets were fixed in 10% neutral buffered formalin and paraffin-embedded. The jejunum of wild-type and MVID pigs were analyzed for the presence of inclusions associated with claudin-2.

### *Immunofluorescence Staining*

**Paraffin-embedded section immunostaining.** Paraffin sections were warmed on a heating block set at 65°C for 10 minutes to facilitate bonding of the tissue with the glass slide. Tissue then was deparaffinized in Histo-Clear (HS-200; National Diagnostics, Atlanta, GA) and a series of ethanol, followed by rehydration and antigen retrieval in citrate buffer (S1699; Dako) in a pressure cooker set for high pressure for 15 minutes. After antigen retrieval, slides were cooled on ice and blocked at room temperature for 1.5 hours with serum-free protein block (X0909; Dako). Mouse on mouse block (MKB-2213; Vector Laboratories, Burlingame, CA) was used for mouse antibodies following the

manufacturer's instructions. Primary antibodies were diluted in antibody diluent with background reducing components (S3022; National Diagnostics) and were incubated overnight at 4°C in a humidified chamber. After 3 washes in PBS for 5 minutes, sections were incubated with secondary antibodies diluted 1:200 in antibody diluent (S0809; Dako, Santa Clara, CA) for 1 hour at room temperature. Hoechst (1:1000 in PBS, 62249, 12.3 mg/mL; Thermo Fisher Scientific) was added to stain the nuclei for 5 minutes. Sections then were washed 3 times in PBS for 5 minutes each. Coverslips were added to sections with ProLong Gold Antifade (P36934; Thermo Fisher Scientific) and allowed to dry before imaging.

**Frozen section immunostaining.** Frozen sections were air dried for 30 minutes before immunostaining to ensure the tissue bonded with the glass slides. After air drying, sections were placed in cold acetone for 1 minute, followed by 1 minute in PBS. Slides then were blocked with 10% normal donkey serum and 0.3% Triton X-100 (Thermo Fisher) in PBS for 1 hour at room temperature. Primary antibodies were diluted in 10% normal donkey serum and 0.3% Triton X-100 in PBS and added to slides in a humidified chamber at 4°C overnight. Next, slides were washed 3 times in PBS for 5 minutes each and then secondary antibodies at 1:200 dilution were added in 0.3% Triton X-100 in PBS at room temperature for 1 hour. Nuclei were stained with 1:1000 dilution of Hoechst for 5 minutes and then slides were washed 3 times in PBS for 5 minutes each. Slides were coverslipped using ProLong Gold Antifade and imaged after drying.

**Primary antibodies.** The following primary antibodies and dilutions were used for immunostaining:

mouse α-p120 1:200 (610133; BD Biosciences, Franklin Lakes, NJ); rabbit α-ezrin 1:200 (3145S; Cell Signaling Technology, Danvers, MA); mouse α-γ-actin 1:100 (sc65638; Santa Cruz Biotechnology, Dallas, TX); rabbit α-α-actinin 4 rabbit 1:200 (ab108198; Abcam, Cambridge, MA); mouse α-Rab11a 1:50 (sc166912; Santa Cruz Biotechnology); rabbit α-Crumb3 1:100 (NBP1-81185; Novus Biologicals, Littleton, CO); mouse α-Pals1 1:200 (sc365411; Santa Cruz Biotechnology); rabbit α-Patj 1:100 (PA5 85444; Thermo Fisher); sheep α-PKCζ/ι 1:500 (AF4465; R&D Systems, Minneapolis, MN); rabbit α-Par3 1:200 (NBP1-88861; Novus Biologicals); rabbit α-Par6 1:200 (ab49776; Abcam); rabbit α-Cdc42 1:100 (ab187643; Abcam); rabbit α-claudin-2 1:30 (Prestige Antibodies HPA051548; Sigma, Saint Louis, MO); rat α-ZO-1 1:200 (MABT11; Millipore, Billerica, MA); rabbit α-ZO-2 1:200 (71140; Invitrogen, Carlsbad, CA); mouse α-occludin 1:200 (33-1500; Invitrogen); and 1:1000 mouse α-cortactin (05-180, clone 4F11; Millipore). For immunostaining of pig intestinal tissues mouse α-γ-actin 1:100 (sc65638; Santa Cruz Biotechnology) and rabbit α-claudin-2 1:30 (Prestige Antibodies HPA051548; Sigma) were used. Secondary antibodies were conjugated to Alexa Fluor 488, Cy3, Alexa Fluor 594, Alexa Fluor 647, or Cy5.

### *Microscope Imaging*

All immunostaining was analyzed using a Zeiss Axio Imager.M2 microscope equipped with an Axiovision digital



imaging system (Zeiss, Oberkochen, Germany) using a 20× objective or a Nikon Ti-E microscope with an A1R laser scanning confocal system (Nikon Instruments, Inc, Melville, NY) using a 60× objective. The Axio imager 20× objective has a Plan-apochromat with a numeric aperture of 0.8 M27. The Nikon A1R 60× oil objective has a Plan apochromat with a numeric aperture of 1.4. Imaging of tissue sections was performed at room temperature and all tissue sections were mounted in ProLong Gold Antifade reagent. The Axio Imager microscope was equipped with an AxioCam HRm Rev.3 camera. The Axiovision digital imaging system was used to export single-channel grayscale TIFF images for all images acquired on the Axio Imager. The Nikon A1R used a Nikon A1 plus camera. Nikon Elements software was used to export images as individual channel TIFF files. Adobe Photoshop (Adobe, San Jose, CA) was used to merge individual channel images into Red Green Blue (RGB).

### SEM Tissue Fracture

To generate SEM images, 5-mm pieces of the most proximal region of the small intestine (duodenum) of Myo5b KO mice were briefly washed in PBS and fixed by immersion in 2.5% glutaraldehyde in 0.1 mol/L cacodylate buffer for 1 hour at room temperature, followed by further fixation at 4°C. The samples were postfixed sequentially in 1% tannic acid, 1% OsO<sub>4</sub>, and 1% uranyl acetate, followed by dehydration in a graded ethanol series. The samples were dried by critical point drying and fractured through the villi using a dulled razor blade. Fractured villi were mounted face up or sideways on carbon tape and sputtered with gold palladium. Scanning electron microscopy was performed on a Quanta 250 FEG at 5 kV (FEI, Lausanne, Switzerland).

### Intestinal Organoid Culture and Differentiation

Proximal small intestinal organoids were generated from neonatal control and Myo5b KO mice following a previously published method.<sup>104</sup> Briefly, the proximal small intestine was excised and the tissue was washed in ice-cold PBS and minced into small pieces using a razor blade. The intestinal pieces were collected in 2 mmol/L EDTA in PBS and incubated at 4°C for 15 minutes on a shaker. After shaking, the EDTA solution was aspirated and replaced with 5 mL of 55 mmol/L D-sorbitol and 34 mmol/L sucrose in PBS. The tissue pieces were shaken in the D-sorbitol and sucrose solution for 1 minute and the supernatant was examined to determine the crypt yield. The suspension of tissue, villi, and crypts in D-sorbitol and sucrose then was passed through a 70-μm strainer (431751; Corning, Corning, NY) and the strained solution containing intestinal crypts was collected for centrifugation. The contents were centrifuged for 5 minutes at 300 × g and the resulting pellet was resuspended in Matrigel (356231; Corning). Thirty microliters of Matrigel-containing crypts were added to wells in a 48-well plate and allowed to polymerize for 30 minutes at 37°C. After polymerization, prewarmed mouse Intesticult media (06000; Stem Cell Technologies, Vancouver, Canada) containing Mycozap (VZA-2031; Lonza, Basel, Switzerland) and

antibiotics was added to wells containing Matrigel domes and crypts. After 2 days in Intesticult media, the medium was replaced with differentiation media, which lacked Wnt to promote enterocyte differentiation. After 3–5 days in differentiation media, intestinal organoids were fixed in 4% paraformaldehyde or 10% neutral buffered formalin for 30 minutes at room temperature, washed twice, and embedded in Histogel (HG-4000-012; ThermoFisher) for paraffin embedding or in optimal temperature compound for frozen sectioning. To inhibit PKC, 10 μmol/L ζ-Stat (DC10984; DC Chemicals, Shanghai, China) was added to Myo5b KO-derived intestinal organoids in the Intesticult media and in the differentiation media so that PKC was inhibited continuously in intestinal organoids during culturing.<sup>105,106</sup> DMSO (1:1000) was added as vehicle control.

### Quantification of Inclusions Associated With Tight Junction Proteins and Statistical Analysis

Intestinal tissue from littermate control and Myo5b KO mice were immunostained for γ-actin and either claudin-2 or ZO-1. Two 20× fields were examined to determine the total number of inclusions that were present at the apical membrane as defined by γ-actin staining. The number of inclusions that were contiguous with the apical membrane and expressed claudin-2 or ZO-1 at the apical membrane over inclusions then were counted. The percentage of inclusions associated with tight junction proteins was calculated by dividing the number of inclusions positive for claudin-2 or ZO-1 at the apical membrane by the total number of inclusions that still were attached to the apical membrane. Four to 5 mice per group were analyzed. Two-way analysis of variance was used to determine significance.

## References

1. Golachowska MR, Hoekstra D, van ISC. Recycling endosomes in apical plasma membrane domain formation and epithelial cell polarity. *Trends Cell Biol* 2010;20:618–626.
2. Roland JT, Bryant DM, Datta A, Itzen A, Mostov KE, Goldenring JR. Rab GTPase-Myo5B complexes control membrane recycling and epithelial polarization. *Proc Natl Acad Sci U S A* 2011;108:2789–2794.
3. Ruemmele FM, Muller T, Schiefermeier N, Ebner HL, Lechner S, Pfaller K, Thoni CE, Goulet O, Lacaille F, Schmitz J, Colomb V, Sauvat F, Revillon Y, Canioni D, Brousse N, de Saint-Basile G, Lefebvre J, Heinz-Erian P, Enninger A, Utermann G, Hess MW, Janecke AR, Huber LA. Loss-of-function of MYO5B is the main cause of microvillus inclusion disease: 15 novel mutations and a CaCo-2 RNAi cell model. *Hum Mutat* 2010;31:544–551.
4. Ruemmele FM, Schmitz J, Goulet O. Microvillous inclusion disease (microvillous atrophy). *Orphanet J Rare Dis* 2006;1:22.
5. Muller T, Hess MW, Schiefermeier N, Pfaller K, Ebner HL, Heinz-Erian P, Ponstingl H, Partsch J, Rollinghoff B, Kohler H, Berger T, Lenhart H, Schlenck B, Houwen RJ, Taylor CJ, Zoller H, Lechner S, Goulet O, Utermann G, Ruemmele FM, Huber LA, Janecke AR. MYO5B

- mutations cause microvillus inclusion disease and disrupt epithelial cell polarity. *Nat Genet* 2008; 40:1163–1165.
6. Davidson GP, Cutz E, Hamilton JR, Gall DG. Familial enteropathy: a syndrome of protracted diarrhea from birth, failure to thrive, and hypoplastic villus atrophy. *Gastroenterology* 1978;75:783–790.
  7. Szperl AM, Golachowska MR, Bruinenberg M, Prekeris R, Thunnissen AM, Karrenbeld A, Dijkstra G, Hoekstra D, Mercer D, Ksiazek J, Wijmenga C, Wapenaar MC, Rings EH, van ISC. Functional characterization of mutations in the myosin Vb gene associated with microvillus inclusion disease. *J Pediatr Gastroenterol Nutr* 2011;52:307–313.
  8. Pohl JF, Shub MD, Trevelline EE, Ingebo K, Silber G, Rayhorn N, Holve S, Hu D. A cluster of microvillous inclusion disease in the Navajo population. *J Pediatr* 1999; 134:103–106.
  9. Erickson RP, Larson-Thome K, Valenzuela RK, Whitaker SE, Shub MD. Navajo microvillous inclusion disease is due to a mutation in MYO5B. *Am J Med Genet A* 2008;146A:3117–3119.
  10. Engevik AC, Coutts AW, Kaji I, Rodriguez P, Ongaratto F, Saqui-Salces M, Medida RL, Meyer AR, Kolobova E, Engevik MA, Williams JA, Shub MD, Carlson DF, Melkamu T, Goldenring JR. Editing myosin VB gene to create porcine model of microvillus inclusion disease, with microvillus-lined inclusions and alterations in sodium transporters. *Gastroenterology* 2020; 158:2236–2249.e9.
  11. Engevik AC, Kaji I, Engevik MA, Meyer AR, Weis VG, Goldstein A, Hess MW, Muller T, Koepsell H, Dudeja PK, Tyska M, Huber LA, Shub MD, Ameen N, Goldenring JR. Loss of MYO5B leads to reductions in Na(+) absorption with maintenance of CFTR-dependent Cl(-) secretion in enterocytes. *Gastroenterology* 2018;155:1883–1897 e10.
  12. Kaji I, Roland JT, Watanabe M, Engevik AC, Goldstein AE, Hodges CA, Goldenring JR. Lysophosphatidic acid increases maturation of brush borders and SGLT1 activity in MYO5B-deficient mice, a model of microvillus inclusion disease. *Gastroenterology* 2020; 159:1390–1405.e20.
  13. Forteza R, Ahsan MK, Carton-Garcia F, Arango D, Ameen NA, Salas PJ. Glucocorticoids and myosin5b loss of function induce heightened PKA signaling in addition to membrane traffic defects. *Mol Biol Cell* 2019; 30:3076–3089.
  14. Kravtsov DV, Ahsan MK, Kumari V, van Ijzendoorn SC, Reyes-Mugica M, Kumar A, Gujral T, Dudeja PK, Ameen NA. Identification of intestinal ion transport defects in microvillus inclusion disease. *Am J Physiol Gastrointest Liver Physiol* 2016;311:G142–G155.
  15. Cutz E, Rhoads JM, Drumm B, Sherman PM, Durie PR, Forstner GG. Microvillus inclusion disease: an inherited defect of brush-border assembly and differentiation. *N Engl J Med* 1989;320:646–651.
  16. Engevik AC, Kaji I, Postema MM, Faust JJ, Meyer AR, Williams JA, Fitz GN, Tyska MJ, Wilson JM, Goldenring JR. Loss of myosin Vb promotes apical bulk endocytosis in neonatal enterocytes. *J Cell Biol* 2019; 218:3647–3662.
  17. Knowles BC, Roland JT, Krishnan M, Tyska MJ, Lapierre LA, Dickman PS, Goldenring JR, Shub MD. Myosin Vb uncoupling from RAB8A and RAB11A elicits microvillus inclusion disease. *J Clin Invest* 2014; 124:2947–2962.
  18. Weis VG, Knowles BC, Choi E, Goldstein AE, Williams JA, Manning EH, Roland JT, Lapierre LA, Goldenring JR. Loss of MYO5B in mice recapitulates microvillus inclusion disease and reveals an apical trafficking pathway distinct to neonatal duodenum. *Cell Mol Gastroenterol Hepatol* 2016;2:131–157.
  19. Whiteman EL, Fan S, Harder JL, Walton KD, Liu CJ, Soofi A, Fogg VC, Hershenson MB, Dressler GR, Deutsch GH, Gumucio DL, Margolis B. Crumbs3 is essential for proper epithelial development and viability. *Mol Cell Biol* 2014;34:43–56.
  20. Charrier LE, Loie E, Laprise P. Mouse Crumbs3 sustains epithelial tissue morphogenesis in vivo. *Sci Rep* 2015; 5:17699.
  21. Gao Y, Lui WY, Lee WM, Cheng CY. Polarity protein Crumbs homolog-3 (CRB3) regulates ectoplasmic specialization dynamics through its action on F-actin organization in Sertoli cells. *Sci Rep* 2016;6:28589.
  22. Loie E, Charrier LE, Sollier K, Masson JY, Laprise P. CRB3A controls the morphology and cohesion of cancer cells through Ehm2/p114RhoGEF-dependent signaling. *Mol Cell Biol* 2015;35:3423–3435.
  23. Lemmers C, Michel D, Lane-Guermonprez L, Delgrossi MH, Medina E, Arsanto JP, Le Bivic A. CRB3 binds directly to Par6 and regulates the morphogenesis of the tight junctions in mammalian epithelial cells. *Mol Biol Cell* 2004;15:1324–1333.
  24. Tepass U. The apical polarity protein network in Drosophila epithelial cells: regulation of polarity, junctions, morphogenesis, cell growth, and survival. *Annu Rev Cell Dev Biol* 2012;28:655–685.
  25. Laprise P, Tepass U. Novel insights into epithelial polarity proteins in Drosophila. *Trends Cell Biol* 2011; 21:401–408.
  26. Gamblin CL, Hardy EJ, Chartier FJ, Bisson N, Laprise P. A bidirectional antagonism between aPKC and Yurt regulates epithelial cell polarity. *J Cell Biol* 2014; 204:487–495.
  27. Michaux G, Massey-Harroche D, Nicolle O, Rabant M, Brousse N, Goulet O, Le Bivic A, Ruemmele FM. The localisation of the apical Par/Cdc42 polarity module is specifically affected in microvillus inclusion disease. *Biol Cell* 2016;108:19–28.
  28. Dhekne HS, Hsiao NH, Roelofs P, Kumari M, Slim CL, Rings EH, van Ijzendoorn SC. Myosin Vb and Rab11a regulate phosphorylation of ezrin in enterocytes. *J Cell Sci* 2014;127:1007–1017.
  29. Bryant DM, Datta A, Rodriguez-Fraticelli AE, Peranen J, Martin-Belmonte F, Mostov KE. A molecular network for de novo generation of the apical surface and lumen. *Nat Cell Biol* 2010;12:1035–1045.

30. Carton-Garcia F, Overeem AW, Nieto R, Bazzocco S, Dopeso H, Macaya I, Bilic J, Landolfi S, Hernandez-Losa J, Schwartz S Jr, Ramon y Cajal S, van Ijzendoorn SC, Arango D. Myo5b knockout mice as a model of microvillus inclusion disease. *Sci Rep* 2015; 5:12312.
31. Sidhaye J, Pinto CS, Dharap S, Jacob T, Bhargava S, Sonawane M. The zebrafish goosepimples/myosin Vb mutant exhibits cellular attributes of human microvillus inclusion disease. *Mech Dev* 2016;142:62–74.
32. Kannan N, Tang VW. Synaptopodin couples epithelial contractility to alpha-actinin-4-dependent junction maturation. *J Cell Biol* 2015;211:407–434.
33. Bretscher A, Weber K. Localization of actin and microfilament-associated proteins in the microvilli and terminal web of the intestinal brush border by immunofluorescence microscopy. *J Cell Biol* 1978; 79:839–845.
34. Lapiere LA, Kumar R, Hales CM, Navarre J, Bhartur SG, Burnette JO, Provance DW Jr, Mercer JA, Bahler M, Goldenring JR. Myosin vb is associated with plasma membrane recycling systems. *Mol Biol Cell* 2001; 12:1843–1857.
35. Nakayama Y, Shivas JM, Poole DS, Squirrell JM, Kulkoski JM, Schleede JB, Skop AR. Dynamins participate in the maintenance of anterior polarity in the *Caenorhabditis elegans* embryo. *Dev Cell* 2009; 16:889–900.
36. Andrews R, Ahringer J. Asymmetry of early endosome distribution in *C. elegans* embryos. *PLoS One* 2007; 2:e493.
37. Balklava Z, Pant S, Fares H, Grant BD. Genome-wide analysis identifies a general requirement for polarity proteins in endocytic traffic. *Nat Cell Biol* 2007; 9:1066–1073.
38. Pieczynski J, Margolis B. Protein complexes that control renal epithelial polarity. *Am J Physiol Renal Physiol* 2011; 300:F589–F601.
39. Margolis B. The Crumbs3 polarity protein. *Cold Spring Harb Perspect Biol* 2018;10:a027961.
40. Fehon RG, McClatchey AI, Bretscher A. Organizing the cell cortex: the role of ERM proteins. *Nat Rev Mol Cell Biol* 2010;11:276–287.
41. Medina E, Williams J, Klipfell E, Zarnescu D, Thomas G, Le Bivic A. Crumbs interacts with moesin and beta(heavy)-spectrin in the apical membrane skeleton of *Drosophila*. *J Cell Biol* 2002;158:941–951.
42. Li Y, Wei Z, Yan Y, Wan Q, Du Q, Zhang M. Structure of Crumbs tail in complex with the PALS1 PDZ-SH3-GK tandem reveals a highly specific assembly mechanism for the apical Crumbs complex. *Proc Natl Acad Sci U S A* 2014;111:17444–17449.
43. Roh MH, Makarova O, Liu CJ, Shin K, Lee S, Laurinec S, Goyal M, Wiggins R, Margolis B. The Maguk protein, Pals1, functions as an adapter, linking mammalian homologues of Crumbs and discs lost. *J Cell Biol* 2002; 157:161–172.
44. Michel D, Arsanto JP, Massey-Harroche D, Beclin C, Wijnholds J, Le Bivic A. PATJ connects and stabilizes apical and lateral components of tight junctions in human intestinal cells. *J Cell Sci* 2005;118:4049–4057.
45. Tan B, Yatim S, Peng S, Gunaratne J, Hunziker W, Ludwig A. The mammalian Crumbs complex defines a distinct polarity domain apical of epithelial tight junctions. *Curr Biol* 2020;30:2791–2804 e6.
46. Hamazaki Y, Itoh M, Sasaki H, Furuse M, Tsukita S. Multi-PDZ domain protein 1 (MUPP1) is concentrated at tight junctions through its possible interaction with claudin-1 and junctional adhesion molecule. *J Biol Chem* 2002;277:455–461.
47. Adachi M, Hamazaki Y, Kobayashi Y, Itoh M, Tsukita S, Furuse M, Tsukita S. Similar and distinct properties of MUPP1 and Patj, two homologous PDZ domain-containing tight-junction proteins. *Mol Cell Biol* 2009; 29:2372–2389.
48. Roh MH, Liu CJ, Laurinec S, Margolis B. The carboxyl terminus of zona occludens-3 binds and recruits a mammalian homologue of discs lost to tight junctions. *J Biol Chem* 2002;277:27501–27509.
49. Fogg VC, Liu CJ, Margolis B. Multiple regions of Crumbs3 are required for tight junction formation in MCF10A cells. *J Cell Sci* 2005;118:2859–2869.
50. Assemat E, Crost E, Ponsere M, Wijnholds J, Le Bivic A, Massey-Harroche D. The multi-PDZ domain protein-1 (MUPP-1) expression regulates cellular levels of the PALS-1/PATJ polarity complex. *Exp Cell Res* 2013; 319:2514–2525.
51. Tamura A, Hayashi H, Imasato M, Yamazaki Y, Hagiwara A, Wada M, Noda T, Watanabe M, Suzuki Y, Tsukita S. Loss of claudin-15, but not claudin-2, causes Na<sup>+</sup> deficiency and glucose malabsorption in mouse small intestine. *Gastroenterology* 2011;140:913–923.
52. Fujita H, Sugimoto K, Inatomi S, Maeda T, Osanai M, Uchiyama Y, Yamamoto Y, Wada T, Kojima T, Yokozaki H, Yamashita T, Kato S, Sawada N, Chiba H. Tight junction proteins claudin-2 and -12 are critical for vitamin D-dependent Ca<sup>2+</sup> absorption between enterocytes. *Mol Biol Cell* 2008;19:1912–1921.
53. Cao H, Orth JD, Chen J, Weller SG, Heuser JE, McNiven MA. Cortactin is a component of clathrin-coated pits and participates in receptor-mediated endocytosis. *Mol Cell Biol* 2003;23:2162–2170.
54. Sauvonnnet N, Dujeancourt A, Dautry-Varsat A. Cortactin and dynamin are required for the clathrin-independent endocytosis of gamma cytokine receptor. *J Cell Biol* 2005;168:155–163.
55. Cao H, Weller S, Orth JD, Chen J, Huang B, Chen JL, Stamnes M, McNiven MA. Actin and Arf1-dependent recruitment of a cortactin-dynamin complex to the Golgi regulates post-Golgi transport. *Nat Cell Biol* 2005; 7:483–492.
56. Katsube T, Takahisa M, Ueda R, Hashimoto N, Kobayashi M, Togashi S. Cortactin associates with the cell-cell junction protein ZO-1 in both *Drosophila* and mouse. *J Biol Chem* 1998;273:29672–29677.
57. Citalan-Madrid AF, Vargas-Robles H, Garcia-Ponce A, Shibayama M, Betanzos A, Nava P, Salinas-Lara C, Rottner K, Mennigen R, Schnoor M. Cortactin deficiency

- causes increased RhoA/ROCK1-dependent actomyosin contractility, intestinal epithelial barrier dysfunction, and disproportionately severe DSS-induced colitis. *Mucosal Immunol* 2017;10:1237–1247.
58. Abe T, La TM, Miyagaki Y, Oya E, Wei FY, Sumida K, Fujise K, Takeda T, Tomizawa K, Takei K, Yamada H. Phosphorylation of cortactin by cyclin-dependent kinase 5 modulates actin bundling by the dynamin 1-cortactin ring-like complex and formation of filopodia and lamellipodia in NG108-15 glioma-derived cells. *Int J Oncol* 2019;54:550–558.
  59. Lee JF, Zeng Q, Ozaki H, Wang L, Hand AR, Hla T, Wang E, Lee MJ. Dual roles of tight junction-associated protein, zonula occludens-1, in sphingosine 1-phosphate-mediated endothelial chemotaxis and barrier integrity. *J Biol Chem* 2006;281:29190–29200.
  60. Yamada H, Abe T, Satoh A, Okazaki N, Tago S, Kobayashi K, Yoshida Y, Oda Y, Watanabe M, Tomizawa K, Matsui H, Takei K. Stabilization of actin bundles by a dynamin 1/cortactin ring complex is necessary for growth cone filopodia. *J Neurosci* 2013;33:4514–4526.
  61. Yamada H, Takeda T, Michiue H, Abe T, Takei K. Actin bundling by dynamin 2 and cortactin is implicated in cell migration by stabilizing filopodia in human non-small cell lung carcinoma cells. *Int J Oncol* 2016;49:877–886.
  62. Chua J, Rikhy R, Lippincott-Schwartz J. Dynamin 2 orchestrates the global actomyosin cytoskeleton for epithelial maintenance and apical constriction. *Proc Natl Acad Sci U S A* 2009;106:20770–20775.
  63. McNiven MA, Kim L, Krueger EW, Orth JD, Cao H, Wong TW. Regulated interactions between dynamin and the actin-binding protein cortactin modulate cell shape. *J Cell Biol* 2000;151:187–198.
  64. Sato T, Vries RG, Snippert HJ, van de Wetering M, Barker N, Stange DE, van Es JH, Abo A, Kujala P, Peters PJ, Clevers H. Single Lgr5 stem cells build crypt-villus structures in vitro without a mesenchymal niche. *Nature* 2009;459:262–265.
  65. Mosa MH, Nicolle O, Maschalidi S, Sepulveda FE, Bidaud-Meynard A, Menche C, Michels BE, Michaux G, de Saint Basile G, Farin HF. Dynamic formation of microvillus inclusions during enterocyte differentiation in munc18-2-deficient intestinal organoids. *Cell Mol Gastroenterol Hepatol* 2018;6:477–493 e1.
  66. Kravtsov D, Mashukova A, Forteza R, Rodriguez MM, Ameen NA, Salas PJ. Myosin 5b loss of function leads to defects in polarized signaling: implication for microvillus inclusion disease pathogenesis and treatment. *Am J Physiol Gastrointest Liver Physiol* 2014;307:G992–G1001.
  67. Simonovic I, Rosenberg J, Koutsouris A, Hecht G. Enteropathogenic *Escherichia coli* dephosphorylates and dissociates occludin from intestinal epithelial tight junctions. *Cell Microbiol* 2000;2:305–315.
  68. McNamara BP, Koutsouris A, O'Connell CB, Nougayrede JP, Donnerberg MS, Hecht G. Translocated EspF protein from enteropathogenic *Escherichia coli* disrupts host intestinal barrier function. *J Clin Invest* 2001;107:621–629.
  69. Shifflett DE, Clayburgh DR, Koutsouris A, Turner JR, Hecht GA. Enteropathogenic *E. coli* disrupts tight junction barrier function and structure in vivo. *Lab Invest* 2005;85:1308–1324.
  70. Guo C, Shen J. Cytoskeletal organization and cell polarity in the pathogenesis of Crohn's disease. *Clin Rev Allergy Immunol* 2020, Epub ahead of print.
  71. Mashukova A, Wald FA, Salas PJ. Tumor necrosis factor alpha and inflammation disrupt the polarity complex in intestinal epithelial cells by a posttranslational mechanism. *Mol Cell Biol* 2011;31:756–765.
  72. Schumann M, Gunzel D, Buergele N, Richter JF, Troeger H, May C, Fromm A, Sorgenfrei D, Daum S, Bojarski C, Heyman M, Zeitz M, Fromm M, Schulzke JD. Cell polarity-determining proteins Par-3 and PP-1 are involved in epithelial tight junction defects in coeliac disease. *Gut* 2012;61:220–228.
  73. Lee M, Vasioukhin V. Cell polarity and cancer—cell and tissue polarity as a non-canonical tumor suppressor. *J Cell Sci* 2008;121:1141–1150.
  74. Dong W, Chen X, Chen P, Yue D, Zhu L, Fan Q. Inactivation of MYO5B promotes invasion and motility in gastric cancer cells. *Dig Dis Sci* 2012;57:1247–1252.
  75. Dong W, Wang L, Shen R. MYO5B is epigenetically silenced and associated with MET signaling in human gastric cancer. *Dig Dis Sci* 2013;58:2038–2045.
  76. Letellier E, Schmitz M, Ginolhac A, Rodriguez F, Ullmann P, Qureshi-Baig K, Frascuilho S, Antunes L, Haan S. Loss of myosin Vb in colorectal cancer is a strong prognostic factor for disease recurrence. *Br J Cancer* 2017;117:1689–1701.
  77. Takei K, Mundigl O, Daniell L, De Camilli P. The synaptic vesicle cycle: a single vesicle budding step involving clathrin and dynamin. *J Cell Biol* 1996;133:1237–1250.
  78. Richards DA, Guatimosim C, Betz WJ. Two endocytic recycling routes selectively fill two vesicle pools in frog motor nerve terminals. *Neuron* 2000;27:551–559.
  79. Clayton EL, Evans GJ, Cousin MA. Bulk synaptic vesicle endocytosis is rapidly triggered during strong stimulation. *J Neurosci* 2008;28:6627–6632.
  80. Clayton EL, Cousin MA. Quantitative monitoring of activity-dependent bulk endocytosis of synaptic vesicle membrane by fluorescent dextran imaging. *J Neurosci Methods* 2009;185:76–81.
  81. Cousin MA. Activity-dependent bulk synaptic vesicle endocytosis—a fast, high capacity membrane retrieval mechanism. *Mol Neurobiol* 2009;39:185–189.
  82. Tapia R, Kralicek SE, Hecht GA. Enteropathogenic *Escherichia coli* (EPEC) recruitment of PAR polarity protein atypical PKCzeta to pedestals and cell-cell contacts precedes disruption of tight junctions in intestinal epithelial cells. *Int J Mol Sci* 2020;21:527.
  83. Kalman D, Weiner OD, Goosney DL, Sedat JW, Finlay BB, Abo A, Bishop JM. Enteropathogenic *E. coli* acts through WASP and Arp2/3 complex to form actin pedestals. *Nat Cell Biol* 1999;1:389–391.
  84. Gruenheid S, DeVinney R, Bladt F, Goosney D, Gelkop S, Gish GD, Pawson T, Finlay BB. Enteropathogenic *E. coli* Tir binds Nck to initiate actin pedestal formation in host cells. *Nat Cell Biol* 2001;3:856–859.

85. Garber JJ, Mallick EM, Scanlon KM, Turner JR, Donnenberg MS, Leong JM, Snapper SB. Attaching-and-effacing pathogens exploit junction regulatory activities of N-WASP and SNX9 to disrupt the intestinal barrier. *Cell Mol Gastroenterol Hepatol* 2018; 5:273–288.
86. Peralta-Ramirez J, Hernandez JM, Manning-Cela R, Luna-Munoz J, Garcia-Tovar C, Nougayrede JP, Oswald E, Navarro-Garcia F. EspF Interacts with nucleation-promoting factors to recruit junctional proteins into pedestals for pedestal maturation and disruption of paracellular permeability. *Infect Immun* 2008;76:3854–3868.
87. Sato T, Mushiake S, Kato Y, Sato K, Sato M, Takeda N, Ozono K, Miki K, Kubo Y, Tsuji A, Harada R, Harada A. The Rab8 GTPase regulates apical protein localization in intestinal cells. *Nature* 2007;448:366–369.
88. Sobajima T, Yoshimura S, Iwano T, Kunii M, Watanabe M, Atik N, Mushiake S, Morii E, Koyama Y, Miyoshi E, Harada A. Rab11a is required for apical protein localisation in the intestine. *Biol Open* 2014;4:86–94.
89. Feng Q, Bonder EM, Engevik AC, Zhang L, Tyska MJ, Goldenring JR, Gao N. Disruption of Rab8a and Rab11a causes formation of basolateral microvilli in neonatal enteropathy. *J Cell Sci* 2017;130:2491–2505.
90. Sakamori R, Das S, Yu S, Feng S, Stypulkowski E, Guan Y, Douard V, Tang W, Ferraris RP, Harada A, Brakebusch C, Guo W, Gao N. Cdc42 and Rab8a are critical for intestinal stem cell division, survival, and differentiation in mice. *J Clin Invest* 2012;122:1052–1065.
91. Melendez J, Liu M, Sampson L, Akunuru S, Han X, Vallance J, Witte D, Shroyer N, Zheng Y. Cdc42 coordinates proliferation, polarity, migration, and differentiation of small intestinal epithelial cells in mice. *Gastroenterology* 2013;145:808–819.
92. Cox CM, Lu R, Salcin K, Wilson JM. The endosomal protein endotubulin is required for enterocyte differentiation. *Cell Mol Gastroenterol Hepatol* 2018;5:145–156.
93. Cox CM, Mandell EK, Stewart L, Lu R, Johnson DL, McCarter SD, Tavares A, Runyan R, Ghosh S, Wilson JM. Endosomal regulation of contact inhibition through the AMOT:YAP pathway. *Mol Biol Cell* 2015; 26:2673–2684.
94. McCarter SD, Johnson DL, Kitt KN, Donohue C, Adams A, Wilson JM. Regulation of tight junction assembly and epithelial polarity by a resident protein of apical endosomes. *Traffic* 2010;11:856–866.
95. Tapia R, Kralicek SE, Hecht GA. EPEC effector EspF promotes Crumbs3 endocytosis and disrupts epithelial cell polarity. *Cell Microbiol* 2017;19:e12757.
96. Harris KP, Tepass U. Cdc42 and Par proteins stabilize dynamic adherens junctions in the *Drosophila* neuroectoderm through regulation of apical endocytosis. *J Cell Biol* 2008;183:1129–1143.
97. Fletcher GC, Lucas EP, Brain R, Tournier A, Thompson BJ. Positive feedback and mutual antagonism combine to polarize Crumbs in the *Drosophila* follicle cell epithelium. *Curr Biol* 2012;22:1116–1122.
98. Roeth JF, Sawyer JK, Wilner DA, Peifer M. Rab11 helps maintain apical crumbs and adherens junctions in the *Drosophila* embryonic ectoderm. *PLoS One* 2009;4: e7634.
99. Ponuwei GA. A glimpse of the ERM proteins. *J Biomed Sci* 2016;23:35.
100. Tilston-Lunel AM, Haley KE, Schlecht NF, Wang Y, Chatterton ALD, Moleirinho S, Watson A, Hundal HS, Prystowsky MB, Gunn-Moore FJ, Reynolds PA. Crumbs 3b promotes tight junctions in an ezrin-dependent manner in mammalian cells. *J Mol Cell Biol* 2016;8:439–455.
101. Cao X, Ding X, Guo Z, Zhou R, Wang F, Long F, Wu F, Bi F, Wang Q, Fan D, Forte JG, Teng M, Yao X. PALS1 specifies the localization of ezrin to the apical membrane of gastric parietal cells. *J Biol Chem* 2005;280:13584–13592.
102. Guan Y, Watson AJ, Marchiando AM, Bradford E, Shen L, Turner JR, Montrose MH. Redistribution of the tight junction protein ZO-1 during physiological shedding of mouse intestinal epithelial cells. *Am J Physiol Cell Physiol* 2011;300:C1404–C1414.
103. Richter KN, Revelo NH, Seitz KJ, Helm MS, Sarkar D, Saleeb RS, D'Este E, Eberle J, Wagner E, Vogl C, Lazaro DF, Richter F, Coy-Vergara J, Coceano G, Boyden ES, Duncan RR, Hell SW, Lauterbach MA, Lehnart SE, Moser T, Outeiro TF, Rehling P, Schwappach B, Testa I, Zapiec B, Rizzoli SO. Glyoxal as an alternative fixative to formaldehyde in immunostaining and super-resolution microscopy. *EMBO J* 2018;37:139–159.
104. Mahe MM, Aihara E, Schumacher MA, Zavros Y, Montrose MH, Helmrath MA, Sato T, Shroyer NF. Establishment of gastrointestinal epithelial organoids. *Curr Protoc Mouse Biol* 2013;3:217–240.
105. Petit I, Goichberg P, Spiegel A, Peled A, Brodie C, Seger R, Nagler A, Alon R, Lapidot T. Atypical PKC-zeta regulates SDF-1-mediated migration and development of human CD34+ progenitor cells. *J Clin Invest* 2005;115:168–176.
106. Ratnayake WS, Apostolatos CA, Apostolatos AH, Schutte RJ, Huynh MA, Ostrov DA, Acevedo-Duncan M. Oncogenic PKC-iota activates Vimentin during epithelial-mesenchymal transition in melanoma; a study based on PKC-iota and PKC-zeta specific inhibitors. *Cell Adh Migr* 2018;12:447–463.

---

Received November 27, 2020. Accepted January 20, 2021.

#### Correspondence

Address correspondence to: Amy C. Engevik, PhD, or James R. Goldenring, MD, Vanderbilt University Medical Center, 2213 Garland Avenue MRB IV 10435, Nashville, Tennessee 37232. e-mail: [amy.c.engevik@vumc.org](mailto:amy.c.engevik@vumc.org) or [jim.goldenring@vumc.org](mailto:jim.goldenring@vumc.org); fax: (615) 322-5209.

#### CRedit Authorship Contributions

Amy C Engevik, PhD (Conceptualization: Lead; Data curation: Lead; Formal analysis: Lead; Funding acquisition: Supporting; Investigation: Lead; Methodology: Lead; Visualization: Lead; Writing – original draft: Lead; Writing – review & editing: Lead)

Evan S Krystofiak (Data curation: Supporting; Methodology: Supporting; Writing – review & editing: Supporting)

Izumi Kaji (Data curation: Supporting; Methodology: Supporting; Writing – review & editing: Supporting)

Anne R Meyer (Data curation: Supporting; Methodology: Supporting)

Victoria G Weis (Conceptualization: Supporting; Writing – review & editing: Supporting)

Anna E Goldstein (Data curation: Supporting; Methodology: Supporting)

Alexander W Coutts (Data curation: Supporting; Methodology: Supporting; Writing – review & editing: Supporting)

Tamene Melkamu (Data curation: Supporting; Methodology: Supporting; Writing – review & editing: Supporting)

Milena Saqui-Salces (Data curation: Supporting; Methodology: Supporting; Writing – review & editing: Supporting)

James Goldenring (Conceptualization: Supporting; Data curation: Supporting; Funding acquisition: Lead; Investigation: Supporting; Resources: Lead; Supervision: Lead; Writing – review & editing: Supporting)

**Conflicts of interest**

The authors disclose no conflicts.

**Funding**

This study was supported by National Institutes of Health grants K01 DK121869 (A.C.E.); R01 DK48370, R01 DK70856, RC2 DK118640 (J.R.G.); and R43 DK109820 (T.M.). Supported by a gift from the Christine Volpe Fund (J.R.G.). This work also was supported by core resources of the Vanderbilt Digestive Disease Center (P30 DK058404), the Vanderbilt-Ingram Cancer Center (P30 CA68485), VU Cell Imaging Shared Resource, and the VUMC Digital Histology Shared Resource (supported by a VA Shared Equipment Grant 1S1BX003097).